4-2016

FERROCENE INCORPORATED INTO POLYURETHANES FOR IMPROVED FLAME-RETARDANT PROPERTIES

Michael Giffin
Pittsburg State University

FERROCENE INCORPORATED INTO POLYURETHANES FOR IMPROVED FLAME-RETARDANT PROPERTIES

A Thesis Submitted to the Graduate School
in Partial Fulfillment of the Requirements
for the Degree of
Master of Science

Michael Giffin

Pittsburg State University

Pittsburg, Kansas

April, 2016

FERROCENE INCORPORATED INTO POLYURETHANES FOR IMPROVED FLAME-RETARDANT PROPERTIES

Michael Giffin

APPROVED:

Thesis Advisor _____
Dr. Charles Neef, Chemistry Department

Committee Member _____
Dr. Petar Dvornic, Chemistry Department

Committee Member _____
Dr. Kristopher Mijares, Chemistry Department

Committee Member _____
Dr. Tim Dawsey, Kansas Polymer Research Center

ACKNOWLEDGEMENTS

I would like to thank my advisor and mentor, Dr. Charles Neef, for his instruction, advice, and correction throughout my educational journey. Without his guidance this thesis would not have been possible. Dr. Neef's contributions in assisting and encouraging my research as well as my goals as I look to the next step in my career are invaluable. Dr. Neef's passion for chemistry inspired me to pursue my graduate degree, and the anticipation of his continued support prompted me to do so at Pittsburg State University.

I appreciate my committee members, Dr. Petar Dvornic, Dr. Tim Dawsey, and Dr. Kristopher Mijares, for being willing to take the time to read, advise, and correct me during the thesis process. I would particularly like to thank Dr. Dawsey and the Kansas Polymer Research Center for allowing me to utilize their laboratory space and testing equipment.

I would like to thank Pittsburg State University Graduate and Continuing studies for funding my position as a graduate teaching assistant, as well as the Chemistry Department for appointing me to it. I am also grateful for the implementation of the Accelerated Master's in Chemistry program so I could complete my degree with greater flexibility.

I would like to thank my wife, Kathryn for her constant support in all my endeavors, particularly her belief in me throughout this entire process. It is her encouragement that always keeps me going when results are not coming in as expected.

FERROCENE INCORPORATED INTO POLYURETHANES FOR IMPROVED FLAME-RETARDANT PROPERTIES

An Abstract of the Thesis by
Michael Giffin

Flame retardant polyurethanes are needed for various commercial and industrial applications; toward that end ferrocene derivatives with multiple hydroxyl groups were synthesized for incorporation into polyurethane thin films for testing. The derivatives synthesized were 2,3-dihydroxypropyl ferrocene carboxylate and di-(2,3-dihydroxypropyl) ferrocene 1-1'-dicarboxylate, which are a diol and a diol, respectively. These compounds were characterized using FT-IR spectroscopy, ^{1}H-NMR and ^{13}C-NMR spectroscopy. These derivatives were incorporated into a commercially available polyol mixture at various weight percentages, mixed with methylene diphenyl diisocyanate, and cast as thin films on glass plates. Each film was tested for flame retardance using a standard burn test chamber and thermal stability in both nitrogen and air. Differential scanning calorimetry and volatile organic compounds testing were also performed on selected films. In addition, potential synergistic effects of the ferrocenyl polyols with triphenylphosphine oxide was studied. These materials were tested using the standard burn test chamber and thermal stability.

TABLE OF CONTENTS

CHAPTER PAGE

1. Introduction……..1
1.1 Flame Retardants and Toxicity……1
1.2 Current Flame Retardants in Polyurethanes……...4
1.3 Previous Studies Using Ferrocene as a Flame Retardant……5
1.4 Project Rationale……. 7

2. Experimental……8
2.1 Materials and Method…… 8
2.2 Synthesis of DFC……... 9
2.3 Synthesis of DHFD…… 9
2.4 Casting of Thin Films…….. 10

3. Results and Discussion…….. 11
3.1 Monomer Synthesis Optimization……... 11
3.2 Monomer Characterization…….. 14
3.3 Polymerization Reactions…… 21
3.4 Thermal Properties…….. 24
3.5 Burn Test……. 30
3.6 VOC Testing…… 34

4. Conclusions……37
4.1 Further Research…….. 38

References……..40

Appendix A- ^{1}H-NMR, ^{13}C-NMR, FT-IR Spectra and DSC……43

Appendix B- VOC Results……52

LIST OF TABLES:

TABLE PAGE

Table 1. GC-MS sample specifications……. 34

LIST OF FIGURES

FIGURE PAGE

Figure 1. FT-IR spectra of DFC at varying reaction times……...12
Figure 2. FT-IR spectra of DFC and DHFD…….15
Figure 3. ^{1}H-NMR spectrum of DFC……....16
Figure 4. ^{1}H-NMR spectrum of DFC with individual integration…….16
Figure 5. ^{13}C-NMR spectrum of DFC……...18
Figure 6. ^{1}H-NMR spectrum of DHFD…….19
Figure 7. ^{13}C-NMR spectrum of DHFD…… 20
Figure 8. TGA of control sample……...24
Figure 9. Plot of TGA char yield versus amount of Fc incorporation……... 25
Figure 10. Plot of TGA 5% weight loss versus amount of Fc incorporation…….26
Figure 11. Plot of TGA 50% weight loss versus amount of Fc incorporation……...26
Figure 12. Contour plot of char yield in air vs % TPO and % DFC……..27
Figure 13. Contour plot of char yield in air vs % TPO and % DHFD……...28
Figure 14. Contour plot of 50% degradation in air vs % TPO and % DFC……...29
Figure 15. Contour plot of 50% degradation in air vs % TPO and % DHFD……... 29
Figure 16. Plot of burn rate versus amount of Fc incorporation……30
Figure 17. Plot of burn distance versus amount of Fc incorporation…….31
Figure 18. Contour plot of burn distance vs % TPO and % DFC……..32
Figure 19. Contour plot of burn distance vs % TPO and % DHFD ……..33
Figure 20. GC of control……35
Figure 21. GC of 30% DFC……... 35

LIST OF SCHEMES

SCHEME PAGE

Scheme 1. Monomers synthesized for polyurethane incorporation……7

Scheme 2. Synthesis of DFC…… 11

Scheme 3. Synthesis of DHFD…….. 14

Scheme 4. Possible isomers from reaction
of ferrocene carboxylic acid and glycidol……....14

Scheme 5. Possible isomers from reaction
of ferrocene dicarboxylic acid and glycidol…….19

Scheme 6. Reaction of 4-4-MDI with a diol……..21

Scheme 7. Reaction of 4-4-MDI with DFC……...22

Scheme 8. Reaction of 4-4-MDI with DHFD……23

LIST OF ABBREVIATIONS

Cp - Cyclopentadienyl

DFC – 2,3-dihydroxypropyl ferrocene carboxylate

DHFD – Di-(2,3-dihydroxypropyl) ferrocene 1-1’-dicarboxylate

DSC – Differential scanning calorimetry

Fc – Ferrocene/ferrocenyl

FCA – Ferrocene carboxylic acid

FDCA – Ferrocene dicarboxylic acid

FR – Flame retardant

IPA – Isopropanol

LOI – Limiting oxygen index

MDI – Methylene diphenyl diisocyanate

MoS – Molybdenum sulfide

PBDEs – Polybrominated diphenyl ethers

TBAB – Tetrabutylammonium bromide

TBAC – Tetrabutylammonium chloride

TGA – Thermogravimetric analysis

THF – Tetrahydrofuran

TLC – Thin layer chromatography

TPO – Triphenylphosphine oxide

VOC – Volatile organic compound

Chapter I

1. Introduction

1.1 Flame Retardants and Toxicity

Polymeric materials require flame retardant (FR) properties for a variety of reasons, depending on the desired application.[1] Due to many polymers being carbon-based, they possess inherent flammability that needs to be addressed, to prevent loss of life and property.[2] Both regulatory agencies and consumers have urged for these materials to be better suited to withstand combustion, while simultaneously being environmentally friendly. The type of FR needed varies with application: building materials and railroad cars require containment of the fire to be the primary goal, while home furnishings and appliances require ignition resistance, and automobiles require escape time to be the most important factor. Other requirements, such as those for aerospace, are more specific, such as low corrosion, thermo-oxidative stability, and many other specific factors, without losing structural properties, and still being cost effective by comparison to metals.

Polyurethanes are produced in a variety of forms, the most notable being rigid foams, flexible foams, surface coatings, and elastomers.[3,4] This class of polymer in general is very flammable and produces heavy smoke upon combustion. Polyurethanes are used as thermal insulation in buildings and transportation, furniture coatings,

cushions, and carpet backing, hardwood floor coatings, and sealants.[4] As is evidenced by the various uses listed above it is of great importance to impede the combustion process and the generation of smoke in those uses, as well as have the products of combustion be non-toxic in the instance of an individual breathing the by-products while escaping a fire.

There are four major types of flame retardant mechanisms:[5] (1) In poisoning/vapor phase, gases are produced that are denser than oxygen so the flame is stifled by this lack of oxygen as well as free-radical interference; this is the main aspect of halogenated flame retardants as well as some phosphine oxides. (2) Dilution occurs as an endothermic reaction takes place alongside combustion which results in a cooling of the overall flame temperature. (3) Char formation occurs as substances burn and create an insulating barrier between the flame and residual material; this has been seen as the primary FR effect of ferrocene containing compounds.[3,6,7] (4) Intumescence creates a charred structure, but has a foaming agent present so that the barrier has more volume and can act as a better barrier for flame and oxygen.

Flame retardant materials are incorporated into polymers by either additive or reactive means, and have a variety of compositions.[1] Additive flame retardants are blended into an existing polymer matrix that does not have the desirable FR characteristics. This is the cheapest method as it does not require new formulations and chemical processes for the polymerization, but problems arise such as compatibility, loss of mechanical strength, and leaching. Reactive flame retardants are bound directly into the polymer chains instead of being blended. This can be achieved through copolymerization with a functionalized FR monomer, or by creating a unique monomer with FR properties. These compounds fit into a variety of classifications, the broadest

distinction being the presence or absence of halogen-containing compounds. Some common halogenated compounds are polybrominated diphenyl ethers (PBDEs), tetrabromophthalate diols and polyethers, derivatives of tetrabromobisphenol acid, chlorinated hydrocarbons, and chlorinated cycloaliphatics.[2] The non-halogenated FRs vary significantly more in their composition and are frequently more environmentally friendly.[5] Phosphorous-based FRs are diverse, including phosphates which promote char, phosphine oxides which react in the vapor phase, inorganic phosphorous such as red phosphorous, and a variety of other derivatives. Metal hydroxides produce water at decomposition temperature, but require significant loading levels which cause the polymer to have significantly less strength. Silicon, Boron, and Nitrogen also act as bases for several other FR materials.[5]

Existing commercial flame retardants used in polymers have come under scrutiny, particularly the halogenated compounds such as PBDEs and chlorinated hydrocarbons.[4,5] While some commercial FRs still use halogenated forms, the industry as a whole is moving away from these compounds to more environmentally friendly non-halogenated alternatives.[5] This trend is due to the toxic nature of the halogenated compounds, which has caused a demand for change from consumers. One of the more common classes of halogenated compounds is PBDEs, which when burned form highly toxic and potentially carcinogenic brominated compounds.[1] A study by the Norwegian Polar Institute[8] gives evidence of bioaccumulation of PBDEs in specific arctic predators, such as glaucous gulls and polar bears. This study also indicated that this buildup may be adversely affecting the animals' thyroid receptors and could be problematic for humans as well. Other studies further condemn PBDEs for causing lowered IQs, attention problems and

other issues in children who were exposed to PBDEs both prenatally and as infants.[9] These, and additional findings, have led many countries, and some states in the U.S.A., to ban PBDEs and/or other halogenated FRs, or to phase them out of production. Other than the problems of specific halogenated compounds, there are two common problems with all of them: They are corrosive to most metals, and upon combustion they produce hydrogen halide acids. These gases are toxic when inhaled, which is particularly problematic in confined spaces.[1] Halogenated FRs can be applied to a variety of polymers with similar effects regardless of the composition of the polymer. However, non-halogenated FRs typically need to be designed for specific classes of polymers as the result is often found to vary with polymer composition.[5] This is largely because the vapor phase mechanism, which is the main type of FR for halogen compounds, is less dependent on polymer composition than other methods. Due to this need for pairing of polymers with effective FRs, ferrocene is being investigated for potential use in polyurethanes.

1.2 Current Flame Retardants in Polyurethanes

There are a variety of both halogenated and non-halogenated FRs currently used for polyurethane foams and films. The materials currently used for polyurethane films vary substantially in type and loading quantity and are in general more effective as a FR in films than in foams due to the fact that foams have more oxygen readily accessible for combustion.[4] Phosphorus compounds are common additives, particularly in combination with other materials, such as 5 wt.% resorcinol bis-diphenylphosphate with 25 wt.% melamine cyanurate, a nitrogen compound. This material has been commercialized by BASF™ as a non-halogenated alternative for FR. Melamine polyphosphate (Melapur®

200, by BASF™) and Aluminum hypophosphite (Phoslite® IP-A by Italmatch Chemicals™) are also used in conjunction with other materials.[5] Aluminum polyphosphate, tris(chloroisopropyl) phosphate and tris(1,3-dichloro-2-propyl) phosphate are also used commonly in polyurethane elastomers.[4]

Halogenated compounds are more common in polyurethane foams than in the films as flame retardance is usually harder to achieve, however both halogenated and non-halogenated FR materials are used in this area as well. Tris(chloroisopropyl) phosphate is used as a main FR material for rigid foams.[5] Brominated diols have also been used as reactive FR materials such as FIREMASTER® 520, a tetrabromophlatate diol produced by Great Lakes.™ PBDEs, as previously discussed, as also used in foams, such as Great Lakes™ DE-61, which contains a blend of PBDEs and phosphate compounds.[4] Many of the FR materials used in films and coatings are also used in foams as well, such as melamine cyanurate, aluminum polyphosphate, as well as others that can be used in either scenario.

1.3 Previous Studies Using Ferrocene as a Flame Retardant

Ferrocene (Fc) has shown potential in previous studies when incorporated into polymers for improving flame retardance.[3,6,7,10] It can be used as an additive filler, without bonding into the polymer structure,[7,10] or it can be bonded directly into the main chains by functionalization into a ferrocene derivative with at least two reactive end groups.[3,6] Ferrocene can create more char when bonded into the backbone of the polymer, but will volatilize less easily and inhibit less in the vapor phase.[3] For ferrocene, bonding into the polymer is preferred, since it is known to sublime at moderate temperatures which would lead to its concentration diminishing over time.[5]

When hydroxyl-terminated block pre-polymers were added to an industrial mixture of methylene diphenyl diisocyanates (MDI), ME-080, in 5, 10, and 15 weight percent increments, the thermogravimetric analysis (TGA) results gave decreasing 10% weight decomposition temperatures, but increasing char yields, with respect to ferrocene pre-polymer weight percent. When tested on a cone calorimeter these compounds showed a decrease in peak heat release rate and total heat released, while being comparable to the control in average heat release rate, and average smoke and carbon monoxide production.[3]

Ferrocene flame retardance has also been shown in the testing of a novel diamine monomer.[6] This monomer contained various functional groups, including amides, ethers, heterocyclic pyridines, ferrocene, and a variable R-group. Limiting oxygen index (LOI) on these polymers was compared to an identical polymer without the ferrocene functionality present. Each comparison resulted in the LOI being between 5% and 5.5% higher for the ferrocene-containing polymer.

A study looking into the synergistic effects of ferrocene (Fc) as a flame retardant with molybdenum sulfide (MoS) found that the two are readily compatible to create nanosheets and contribute to flame retardance in polystyrene more than either compound individually.[7] This study found both decomposition temperature and char yield for the MoS-Fc significantly higher than the control polystyrene, while the ferrocene addition increased char yield but had minimal positive effect on decomposition temperature.

The effect of ferrocene in the vapor phase has also been investigated.[10] Sublimation of ferrocene into the air surrounding a burning sample, measured a normalized burning velocity of 0.45 at 400ppm ferrocene in the air relative to no

ferrocene present. These studies have given a variety of results, but all with promising potential for ferrocene as a flame retardant, showing primarily char formation, but also vapor phase, as the method of flame suppression.

1.4 Project Rationale

With the previous promising results of ferrocene as a flame retardant, the goal of this research was to incorporate novel ferrocene derivatives into a standard polyurethane film and determine their potential as FR using a burn test, thermogravimetric analysis, differential scanning calorimetry, as well as volatile organic compound testing. Ferrocene derivatives synthesized were 2,3-dihydroxypropyl ferrocene carboxylate (DFC) and di-(2,3-dihydroxypropyl) ferrocene 1-1'-dicarboxylate (DHFD), which are a diol and a tetraol, respectively. These monomers are shown below in Scheme 1.

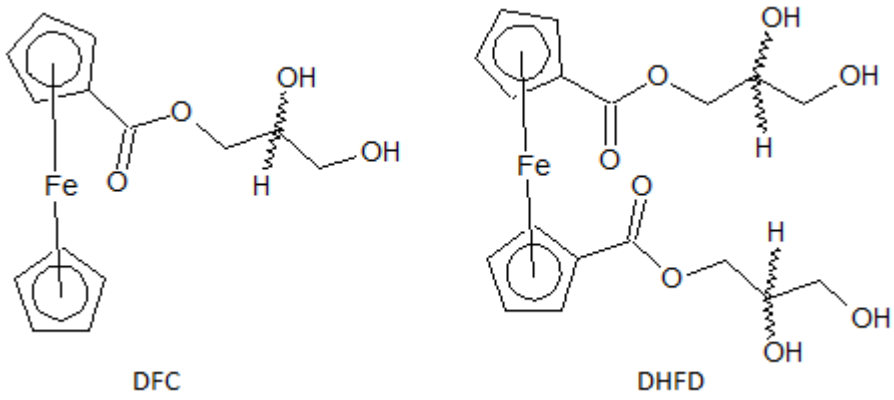

Scheme 1. Monomers synthesized for polyurethane incorporation.

These ferrocenyl derivatives bond directly into the polyurethane films by the hydroxyl functional groups, and add flame retardant properties to the polymer. In addition, triphenylphosphine oxide (TPO) was added into the ferrocene-containing polyurethane films to investigate synergistic effects.

Chapter II

2. Experimental

2.1 Materials and Methods

All starting materials were commercially available unless specified otherwise. Ferrocene carboxylic acid (FCA) was synthesized in 85.0% overall yield according to the literature method.[11] Ferrocene was reacted with 2-chlorobenzoyl chloride under Friedel-Crafts conditions followed by conversion to ferrocene carboxylic acid using water and potassium tert-butoxide. Ferrocene dicarboxylic acid (FDCA) was synthesized in 82.0% overall yield according to the literature method.[12,13] Ferrocene was converted to 1,1'-diacetyl ferrocene under Friedel-Crafts conditions followed by oxidization to ferrocene dicarboxylic acid using sodium hypochlorite. Polyol mixture and methylene diphenyl diisocyanate (MDI) for polyurethane films were provided by ETCO-Specialty Products Inc. in Girard, Kansas.

Characterization of the monomer products was achieved using a Bruker Ultrashield™ 300MHz NMR spectrometer for both ^{13}C and ^{1}H spectra. Infrared spectra of the monomers were taken on a Perkin-Elmer Spectrum Two™ FT-IR L1600400 spectrometer. For the polymer films, thermogravimetric analysis was performed on a TGA-Q50, and differential scanning calorimetry was performed on a DSC-Q100, both products of TA™ Instruments. Standard burn tests were performed in an SDL-Atlas™

vertical flame chamber, M223M. Testing for volatile organic compounds (VOCs) was performed on a gas chromatography-mass spectrometer GCMS-QP210SE which was made by Shimadzu.™

2.2 Synthesis of DFC

To a 500mL round bottom flask were added isopropanol (IPA) (300ml), FCA (16.25 g, 70.64 mmol) and tetrabutylammonium chloride (TBAC) (0.3950 g, 1.42 mmol) and a nitrogen atmosphere was established. Glycidol (5.23 g, 70.60 mmol) was added to the mixture and then the reaction was heated to reflux and stirred for 16.5 hours. Upon completion, activated charcoal was added to the reaction flask, and its contents were vacuum filtered through Celite® in a glass sintered funnel. The product was dried over magnesium sulfate and solvent was removed resulting in 95.5% yield of 2,3-dihydroxypropyl ferrocene carboxylate (DFC). ^{1}H NMR (DMSO, δ.ppm): 4.769, 4.694, 4.482 and 4.424 (4H on sub. Cp-ring), 4.247 and 4.212 (5H on unsub. Cp-ring), 4.169, 4.081, 3.747 and 3.458 (5H on alkyl chain). ^{13}C NMR (DMSO, δ.ppm): 170.651, 71.279, 70.962, 70.779, 69.903, 69.801, 69.629, 69.555, 69.426, 65.235, 62.741. IR (solid, cm^{-1}): 3392.24 (O-H), 3107.50 (=C-H), 2946.33 and 2884.00 (-C-H, alkane chain), 1688.19 (C=O).

2.3 Synthesis of DHFD

Di-(2,3-dihydroxypropyl) ferrocene 1-1'-dicarboxylate (DHFD) was synthesized from ferrocene dicarboxylic acid in the same manner as DFC in this work. For the large scale synthesis, the amounts used were as follows: IPA (220ml), FCA (10.79 g, 39.4 mmol), TBAC (0.263 g, 0.946 mmol), and glycidol (6.91 g, 93.3 mmol). Reflux time was

23.5 hours and the workup was the same as DFC. The reaction resulted in 87.0% yield. ^{1}H NMR (DMSO, δ.ppm): 5.300-4.300 (8H on Cp-rings), 4.250-3.200 (10H on alkyl chain). ^{13}C NMR (DMSO, δ.ppm): 169.669, 75.678, 73.091, 72.599, 71.310, 71.047, 70.909, 69.497, 65.583, 63.310, 62.747, 62.126, 61.823. IR (liquid film, cm^{-1}): 3365.81 (O-H), 3112.40 (=C-H), 2939.83 and 2881.40 (C-H, alkane chain), 1691.41 (C=O).

2.4 Casting of Thin Films

Polyurethane films for control samples were cast with an 8:2 ratio (w/w) of polyol mixture to MDI. For polyurethane films containing DFC, the amount of MDI was determined based upon the amount of polyol (8:2 ratio (w/w) of polyol mixture to MDI) and the amount of DFC (8:5 ratio (w/w) of DFC to MDI). For polyurethane films containing DHFD, the same polyol to MDI ratio was used however the ratio of DHFD to MDI used was 8:7 (w/w). These ratios were used to give equimolarity of reacting functional groups in the polyurethane. For DFC, a mortar and pestle were used to grind the monomer prior to mixing. In cases where triphenylphosphine oxide (TPO) was incorporated, TPO amounts were relative to the combined weight of the polyols and MDI. All films had 4mL of acetone added to the mixture to dissolve the ferrocene derivatives and/or the TPO. Components of the films were mixed together without MDI, which was then added to the mixture and stirred for 45-60 seconds. This mixture was then poured onto glass plates and cast using a doctor blade for consistent thickness, allowed to sit at room temperature for two to four hours, and placed in an oven overnight at 66°C. Films were cut to make four films of dimensions 5 by 1.25 inches, of a as well as excess small pieces for use in thermal testing.

Chapter III

3. Results and Discussion

3.1 Monomer Synthesis Optimization

Optimization of monomer synthesis was initially performed for DFC, then applied to the synthesis of DHFD. The optimized reaction scheme of DFC is shown in Scheme 2.

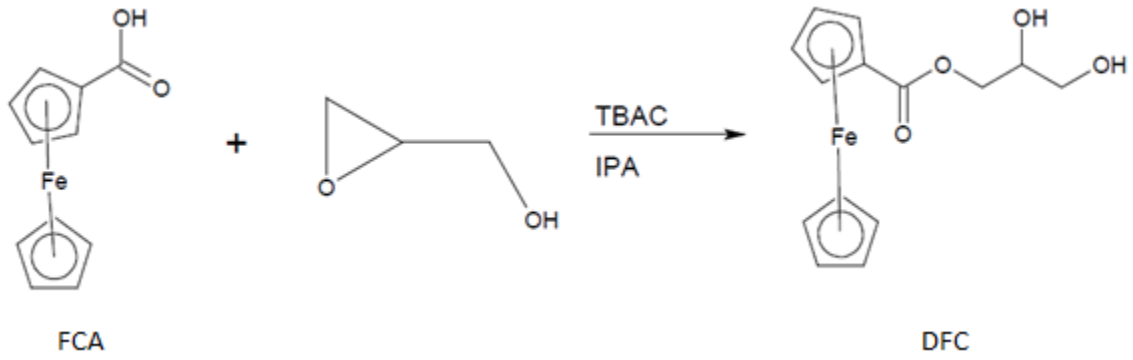

Scheme 2. Synthesis of DFC

DFC was first synthesized in tetrahydrofuran (THF) with tetrabutylammonium bromide (TBAB) as the catalyst for 14 hours.[14] After several unsuccessful purification attempts of the crude DFC, the synthesis was optimized to minimize side reactions and produce a product requiring less extensive purification. The reaction was run simultaneously with four different solvent/catalyst combinations. IPA and THF were the solvents used while TBAB and TBAC were the catalysts, at 3 mol%. FT-IR spectra were taken at intervals throughout each reaction for each combination, as well as thin layer chromatography

(TLC) at the perceived endpoint of the reaction. A sampling of FT-IR spectra taken at varying intervals for the IPA/TBAC combination is shown in Figure 1. These samples were taken by attenuated total reflectance after the solvent had evaporated. The remaining spectra for the other combinations are located in Appendix A, Figures S1-S3.

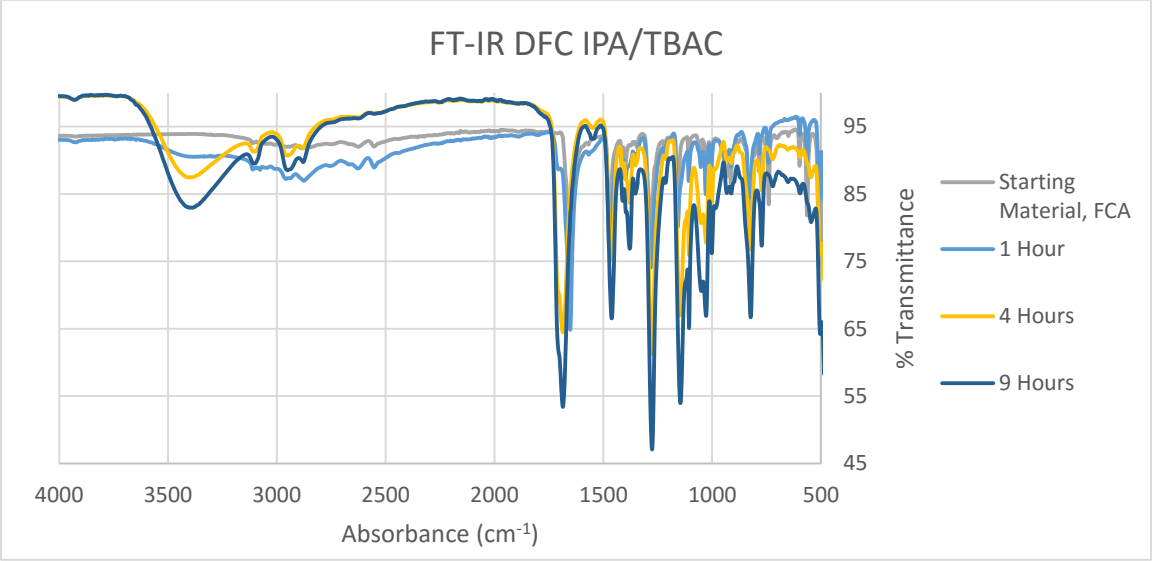

Figure 1. FT-IR spectra of DFC at varying reaction times

The slight shift in the carbonyl peak (1652cm^{-1} to 1688cm^{-1}) and the appearance of the hydroxyl peak (3392cm^{-1}) were monitored throughout the reaction by taking samples from the reaction vessel at each hour. This change in wavenumber of the carbonyl peak is due to the conversion of the carboxylic acid carbonyl into an ester carbonyl, which would have slightly different vibrational frequencies. As the reaction neared completion, the carbonyl peak's progression halted, as did the increase in the hydroxyl peak. On comparison with previous FT-IR spectra taken on the final product of DFC, these spectra were identical. The completion of the reaction was further confirmed for each of the reactions by performing TLC in a 1:1 ratio of ethyl acetate to hexane which resulted in only one spot with retention value of 0.9 versus 1.0 for the original FCA. The other

reactions were found to be less efficient due to the need for a greater reaction time than IPA/TBAC, or resulting in side products evident by the appearance of vinyl peaks in the ^{1}H-NMR spectra after the reactions were completed. TLC on these compounds was inconclusive however with regard to the purity of the compounds. Due to these factors, it was concluded that the IPA/TBAC combination was most effective and resulted in the optimal product with 95.5% yield.

The ideal amount of the TBAC catalyst to be used was also optimized by testing 1, 2, 3, or 4 mol%. The reactions were monitored by FT-IR and TLC using the same process as previously described. Each reaction was monitored until completion, as determined by the shifting of the carbonyl peak and the appearance of only one spot on the TLC plates. ^{1}H-NMR spectra of the samples were taken, which resulted in the 3 and 4 mol% reactions being eliminated due to additional peaks in the spectra that were unexpected. 1 mol% was determined not to be practical as the required reaction time for completion was extensive. The remaining trial of 2 mol% TBAC at 16.5 hours was determined to be ideal for the reaction. The FT-IR spectrum of 2 mol% IPA/TBAC DFC synthesis is Appendix A, Figure S4.

The synthesis conditions for DHFD were based on the DFC reaction parameters. The optimized synthesis of DHFD is shown in Scheme 3 on the following page.

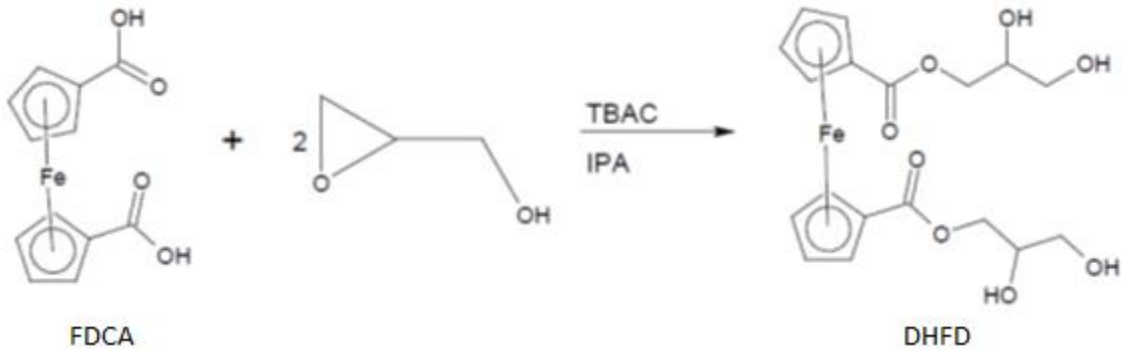

FDCA DHFD

Scheme 3. Synthesis of DHFD

The synthesis of DHFD was also performed in IPA with TBAC as the catalyst with the only variation being the doubling of the molar ratio of glycidol. The time of the reaction was determined using FT-IR and TLC as previously explained, resulting in a final reaction time of 23.5 hours and 87.0% yield.

3.2 Monomer Characterization

The synthesis of DFC can produce two products, depending on the carbon attacked in the reaction. The two possible isomers are shown below in Scheme 4, with the waved lines indicating unknown stereochemistry.

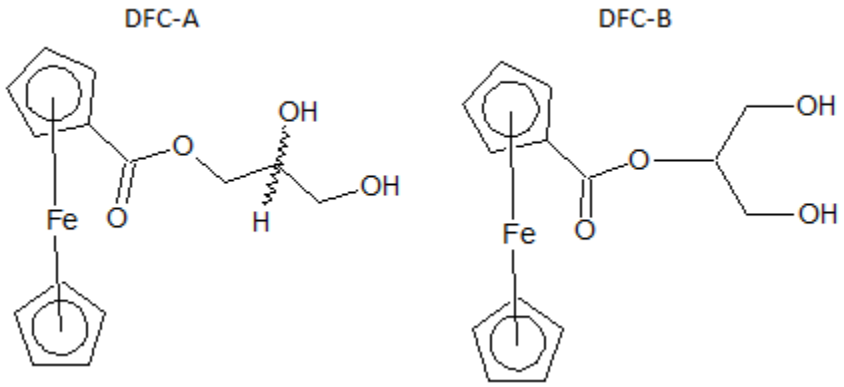

Scheme 4. Possible isomers from reaction of ferrocene carboxylic acid and glycidol

In addition to the two isomers, on DFC-A there is the possibility of both R and S enantiomers around the secondary carbon with the hydroxyl group.

FT-IR spectra of the DFC and DHFD monomers are shown below in Figure 2.

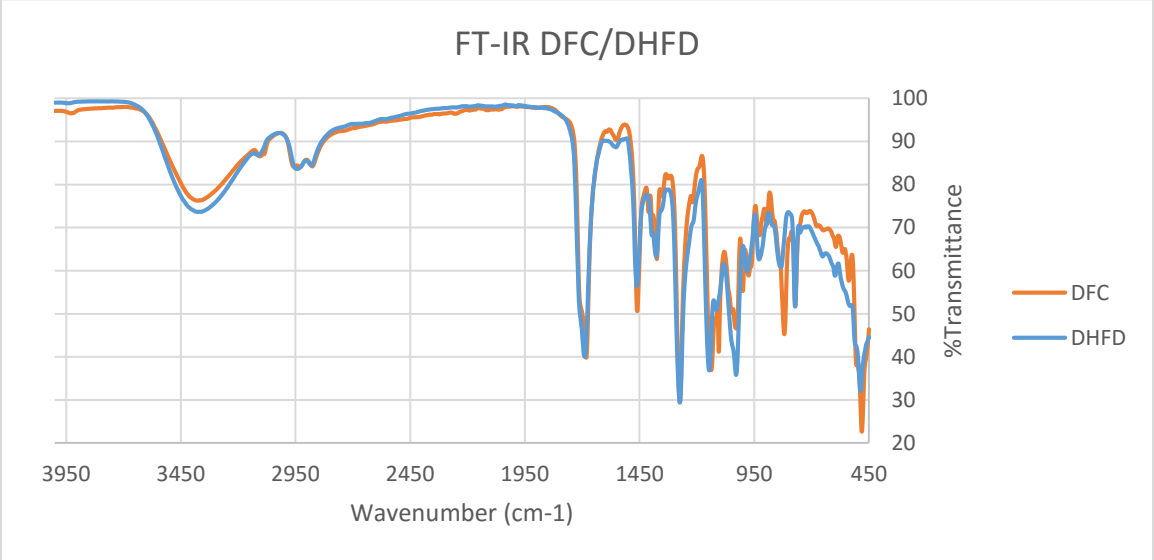

Figure 2. FT-IR spectra of DFC and DHFD

The functional groups, hydroxyl and carbonyl, are consistent between the two monomer spectra, with only minor increases in intensity between the two spectra on the carbonyl and hydroxyl peaks, as would be expected.

The ^{1}H-NMR spectrum of the DFC shows 10 signals, the solvent peak (DMSO) at 2.505ppm as well as a peak from residual IPA at 1.057ppm. Other peaks in the 0-1.750ppm range are likely due to minor amounts of aliphatic impurities. The relevant portion of the spectrum is shown on the following page in Figure 3, with the full spectrum as an inset, while the full spectrum is shown in more detail in Appendix A, Figure S5. Individual integration of these peaks is shown in Figure 4 on the following page.

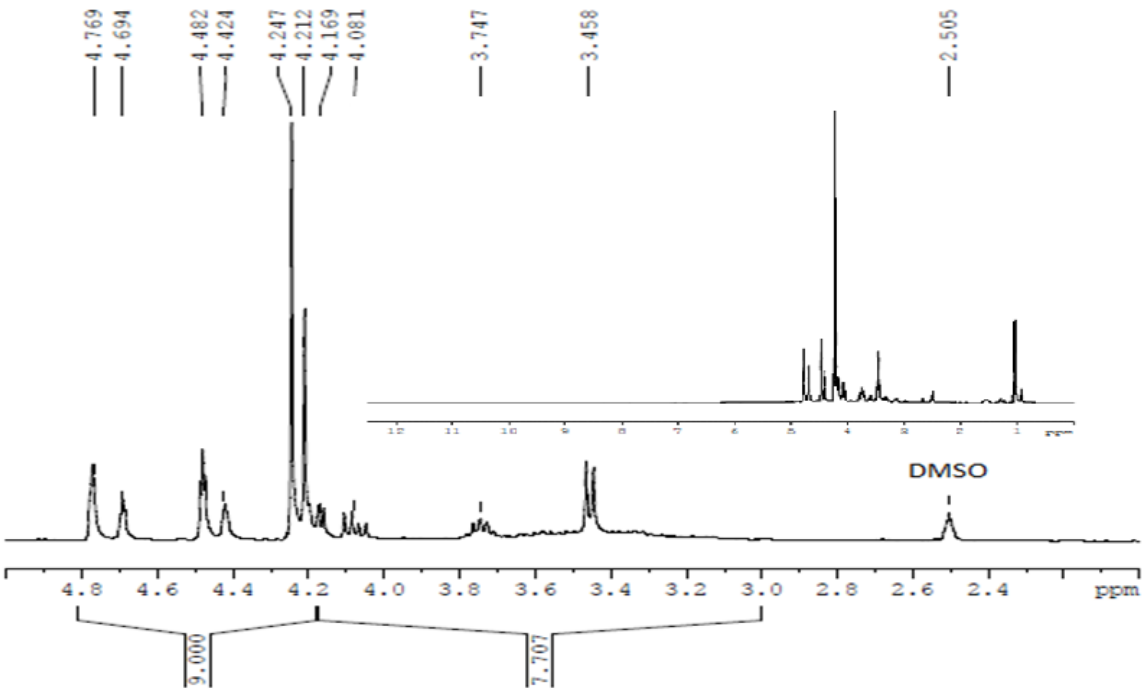

Figure 3. ^{1}H-NMR spectrum of DFC

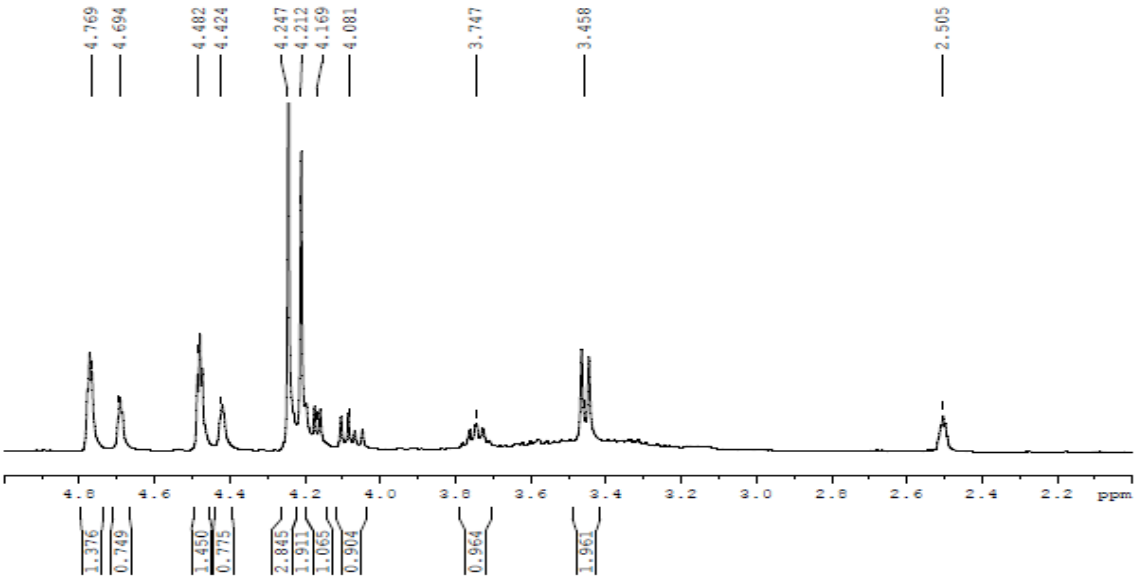

Figure 4. ^{1}H-NMR spectrum of DFC with individual integration

Each of the peak pairs, centered at 4.750ppm, 4.350ppm and 4.230ppm, from the ferrocenyl protons are from the same protons on DFC-A and DFC-B. Integration of each

of these peaks, shown in Figure 4, gives a ratio of the isomers to each other, resulting in 1.83 for peaks at 4.750ppm and 1.87 for peaks at 4.350ppm. The ratio of the peaks at 4.230ppm results in a lower value of 1.49, but this discrepancy can be contributed to coincidental overlap of the downfield ferrocenyl peak with an aliphatic proton peak. Due to these integrations, the isomer ratio would fall near 1.85, although it is not known which regioisomer is favored. The absence of a carboxylic acid peak in the 10-12ppm range confirms complete conversion of FCA, as previously indicated from the FT-IR and TLC. Hydroxyl protons are often not visible in distinct peaks due to proton exchange, and often show up in the baseline over a certain range.[15] For this reason, broad integration was performed on the ferrocenyl and aliphatic regions of the spectrum, resulting in a 9.0 to 7.7 ratio. The theoretical ratio of these regions would be 9 to 7, but this increase in the aliphatic range can be attributed to water remaining in the sample that would also be present in the same range of the baseline.

^{13}C NMR of the DFC resulted in 10 prominent signals in addition to the solvent peak of DMSO at 39.500ppm. The relevant portions of the spectrum are shown on the following page in Figure 5. The full spectra is in Appendix A, Figure S6.

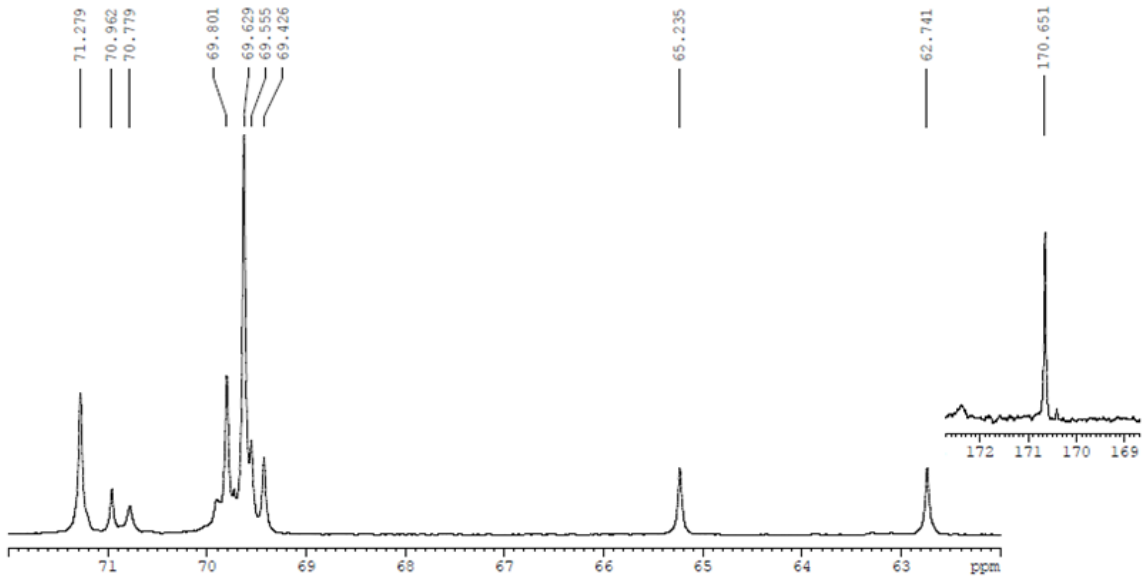

Figure 5. ^{13}C-NMR spectrum of DFC

The only peak which can be attributed to a carbon with certainty present is that of the carbonyl at 170.651ppm. The other 9 peaks account for the expected 7 remaining differing carbons on DFC-A and an additional 2 differing carbons on DFC-B.

The ^{1}H-NMR spectrum of DHFD was even more difficult to interpret due to the increase in possible isomers. This is due to the expected presence of diastereomers as well as regioisomers. The three regioisomers of DHFD are shown on the following page in Scheme 5, with the stereocenter bonds shown by waved lines.

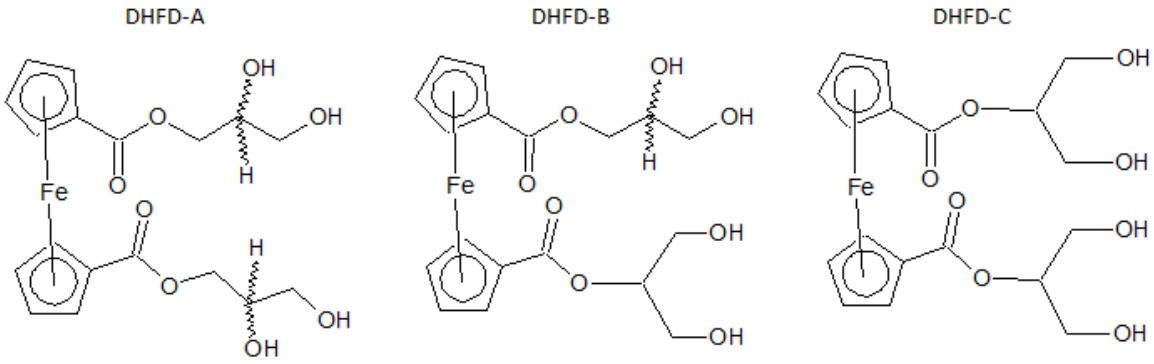

Scheme 5. Possible isomers from reaction of ferrocene dicarboxylic acid and glycidol

IPA and DMSO appear in the DHFD spectrum in the same locations as in the DFC spectrum. Similarly the relevant portion for DHFD is shown below in Figure 6, with the full spectrum as an inset, and shown in more detail in Appendix A, Figure S7.

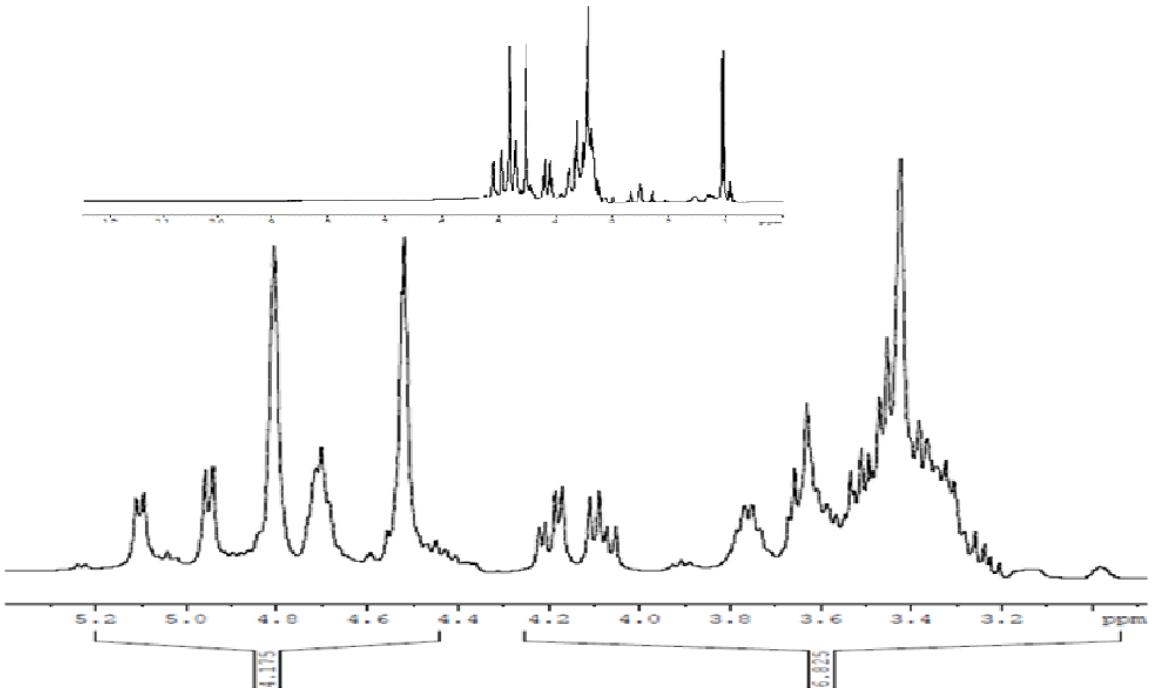

Figure 6. ^{1}H-NMR spectrum of DHFD

As is evident by the abundance of peaks and unclear splitting patterns, the combination of three regioisomers and diastereomers in DHFD-A and DHFD-B leads to a very

complicated spectrum. The broad integration yielded a ratio of 4.18 to 6.83 consistent with the theoretical integration of ferrocenyl to aliphatic peaks and alcohols which is 4 to 7. As was the case with DFC, the absence of the carboxylic acid peak between 10 and 12ppm confirmed the compete conversion of FDCA to DHFD.

^{13}C NMR of the DHFD resulted in 12 signals in addition to the solvent peak. The relevant portions of the spectrum are shown below in Figure 7. The full spectrum is in Appendix A, Figure S8.

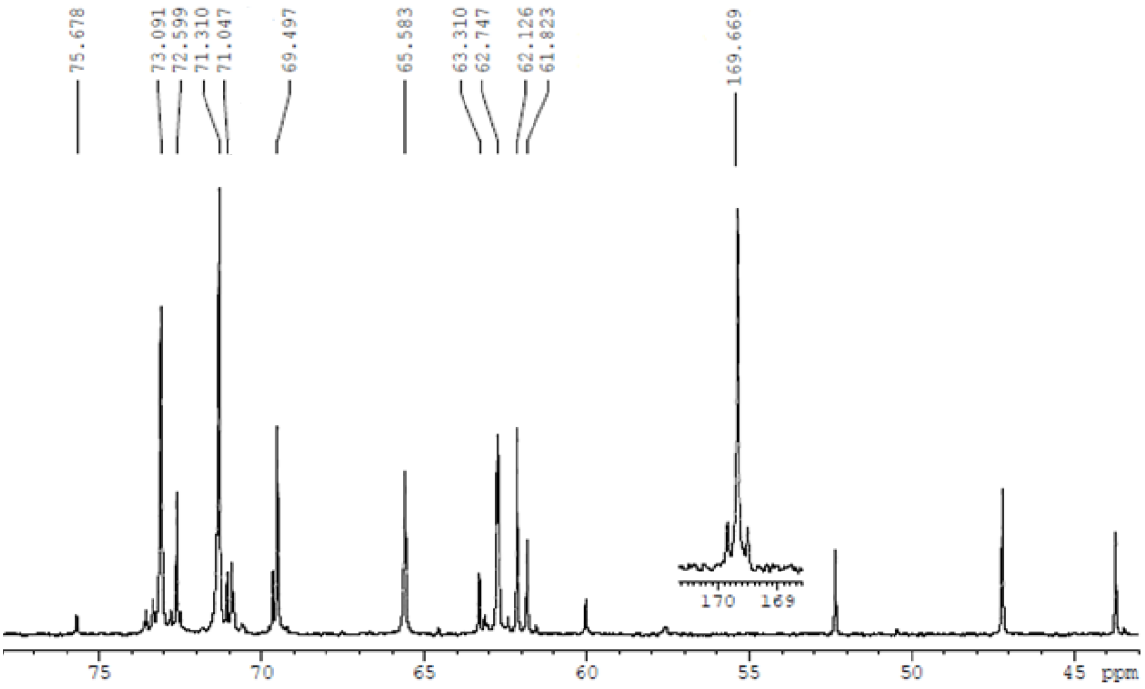

Figure 7. ^{13}C-NMR spectrum of DHFD

As with DFC, the easily identifiable peak is the carbonyl at 169.669. As there were some impurities in the proton spectrum for DHFD it would be expected to see some evidence in the carbon as well. The peaks below 60.500ppm were dismissed as likely impurities due to the expected range of shifts for the compound. The remaining 11 peaks would

correlate to the 11 types of carbons on DHFD-B. Assuming carbons do not change shift significantly through the central iron atom, then DHFD-A and DHFD-C would have the same shifts for the respectively similar carbons.

Unfortunately there is little clarity in the characterization of these monomers due to the presence of regioisomers and diastereomers. However focus was given to the functionality of the monomers in polyurethanes as a flame retardant rather than purification and characterization of isomers. DFC and DHFD stereochemistry should have no effect on the bonding into polyurethanes, although the isomers may have some effect as the secondary alcohols would be less reactive than primary alcohols. An attempt was made to separate the isomers using column chromatography. It was determined that the compound reacted on the column if eluted slowly enough to separate the isomers, so this was dismissed for the sake of practicality.

3.3 Polymerization Reactions

The reaction of the 4-4-MDI, which is one of the components of the MDI mixture used, with a diol in the polyol mixture to create a polyurethane is shown in Scheme 6 below.

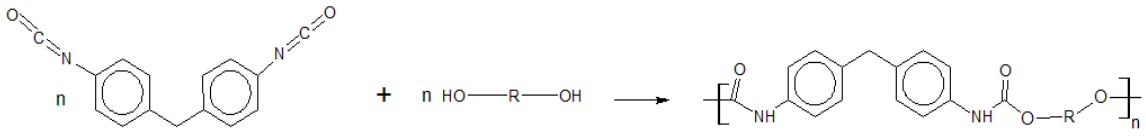

Scheme 6. Reaction of 4-4-MDI with a diol

This reaction shows the formation of a standard urethane linkage by the reaction of a hydroxyl group with an isocyanate, with water being produced as a byproduct. The

R-group in this reaction is unknown as the polyol mixture is a combination of diols and triols and the exact components are not available as it is proprietary knowledge.

The reaction of 4-4-MDI with DFC is shown below in Scheme 7.

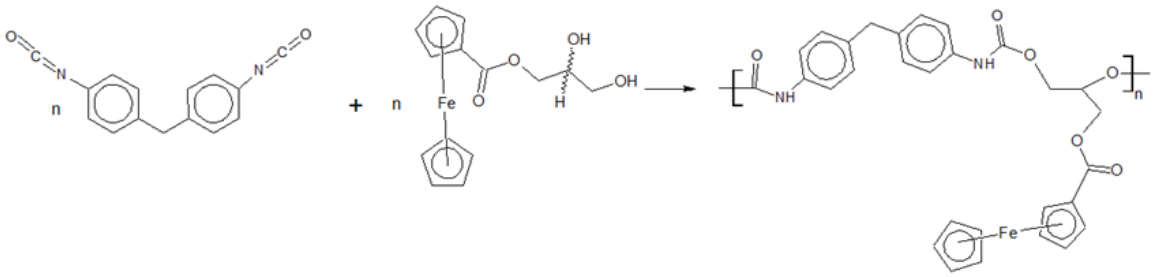

Scheme 7. Reaction of 4-4-MDI with DFC

This reaction scheme shows the repeat unit resulting from the polymerization of MDI with the DFC monomer. This reaction occurs in conjunction with the reactions given by Scheme 6, the reaction of MDI with the polyol mixture. The resulting DFC-containing thin film would have these Fc-containing repeat units interspersed in the polymer, which appears to have a random distribution with the polyol repeat units based on appearance as well as the fact that the hydroxyl groups should be similarly reactive.

The reaction of 4-4-MDI with DHFD is shown on the following page in Scheme 8.

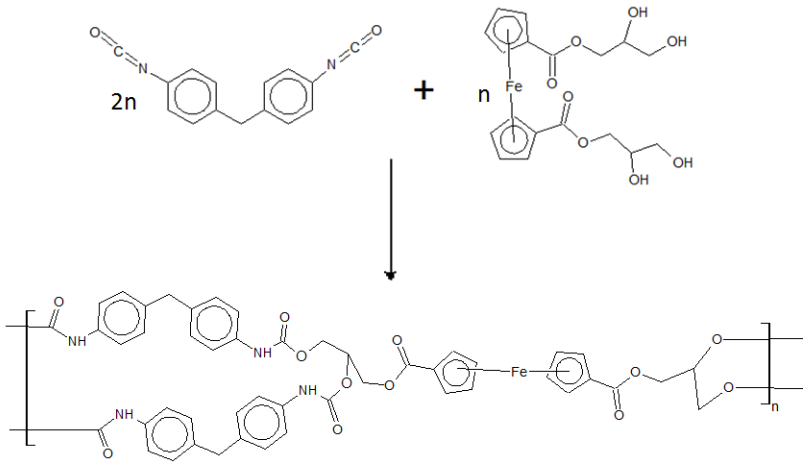

Scheme 8. Reaction of 4-4-MDI with DHFD

Unlike the DFC polymerization, this reaction adds to the density of crosslinking in the polymer as the DHFD monomer has four reactive hydroxyl groups instead of the two of DFC, which only result in increasing chain length. This was seen in a slightly increased rigidity of the DHFD-containing thin films by comparison to the control films or to the DFC-containing films. As with the DFC, this DHFD repeat unit would only account for a portion of the polymer and is also expected to be a random copolymer with the polyol repeat units.

In addition to these reactions there is also the possibility of urea linkages being formed in the case of a slightly higher ratio of isocyanate functional groups to hydroxyl groups. This would result in the formation of a urea with water in the atmosphere, followed by the release of carbon dioxide, converting the urea to an amine, which would react with another isocyanate to form the urea linkage. These should be minimal as equimolarity of functional groups was attempted, however some urea is expected.

3.4 Thermal Properties

Ferrocene was incorporated into a standard polyurethane film at 10%, 20%, and 30% (w/w) with both DFC and DHFD monomers. This loading ratio is based on the final mass of the polymerization mixture of polyol, MDI, and Fc or TPO if these additives were incorporated. Differential scanning calorimetry (DSC) was performed on the samples containing ferrocene (Fc) monomers, however no significant change in glass transition temperature was observed between these samples and a control sample polyurethane film which contained no Fc monomers or TPO. These DSC results are in Appendix A, Figures S9-S15.

These films were also tested for thermal stability using thermogravimetric analysis (TGA), both in air and in nitrogen. The TGA of the control polyurethane thin film, containing no additives, is shown below in Figure 8.

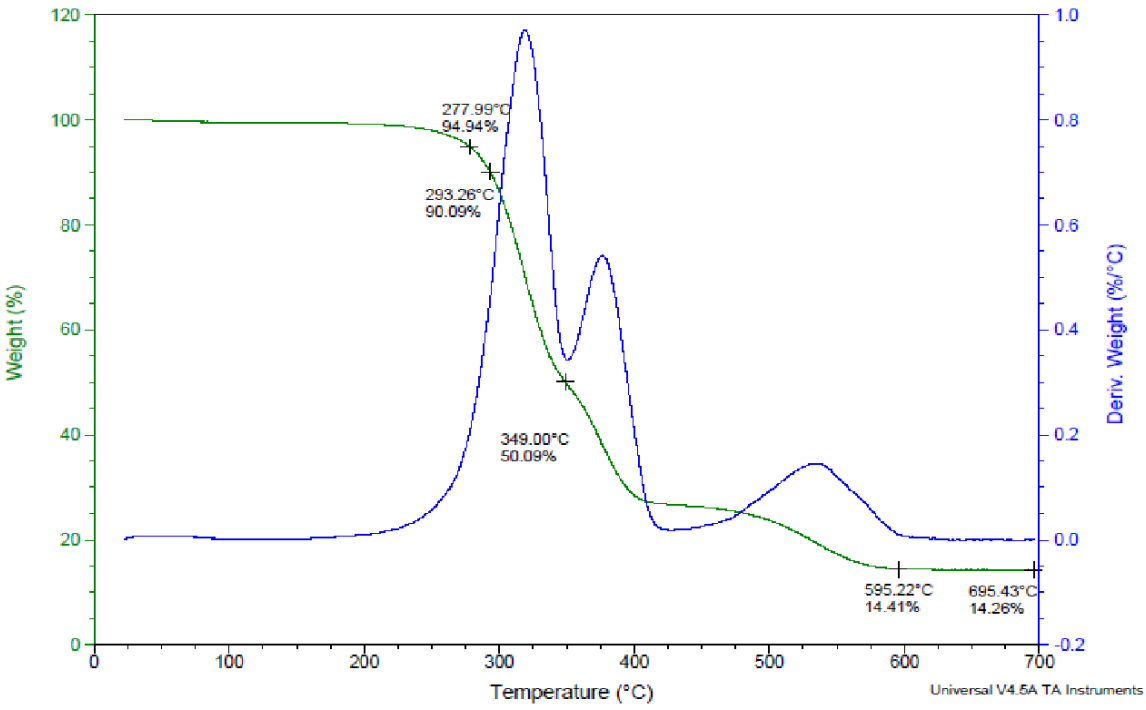

Figure 8. TGA of control sample

The above TGA is shown as an example of the gradual degradation of the polymer under thermo-oxidative stress. All of the samples tested using TGA had results showing similar patterns in degradation with an increase in temperature, although characteristic values differed slightly with each sample. The temperatures at which 5% and 50% of the mass was lost were used as determining values of thermal stability along with the char yield at the end of the run at 600°C. Figure 9 shows the trends in char in both air and nitrogen on the following page with respect to the quantity of Fc incorporation, which is the percent loading of DFC or DHFD.

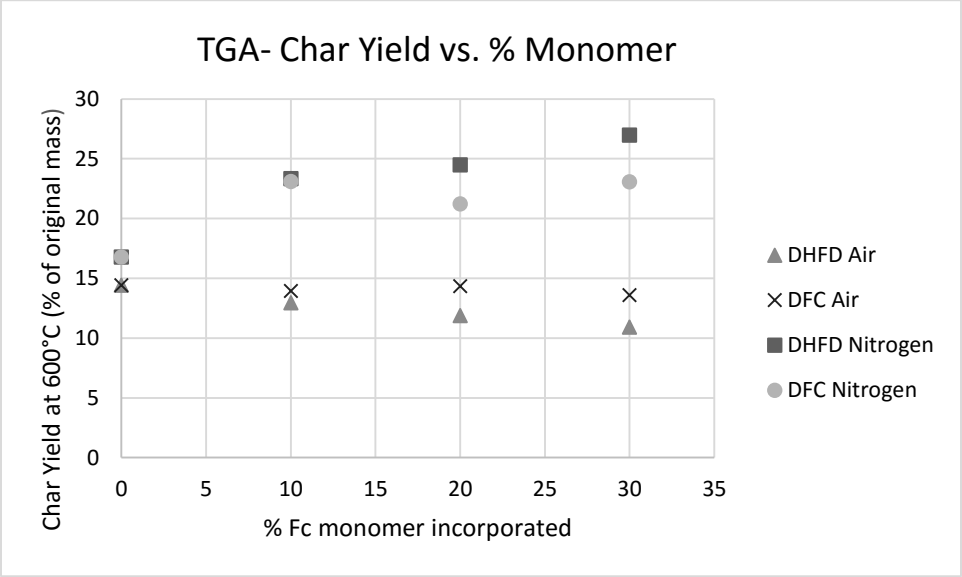

Figure 9. Plot of TGA char yield versus amount of Fc incorporation

As evident in Figure 9, for TGA performed in nitrogen there was an increase in char yield for both monomers as the amount of ferrocene increased. In contrast, the char yield slightly decreased in air as the amount of ferrocene increased. This suggests that some of the Fc bonding in the polymer was not as thermo-oxidatively stable as the parent

polymer. Figures 10 and 11 below show respectively the 5% degradation temperature in nitrogen and air and the 50% degradation in air.

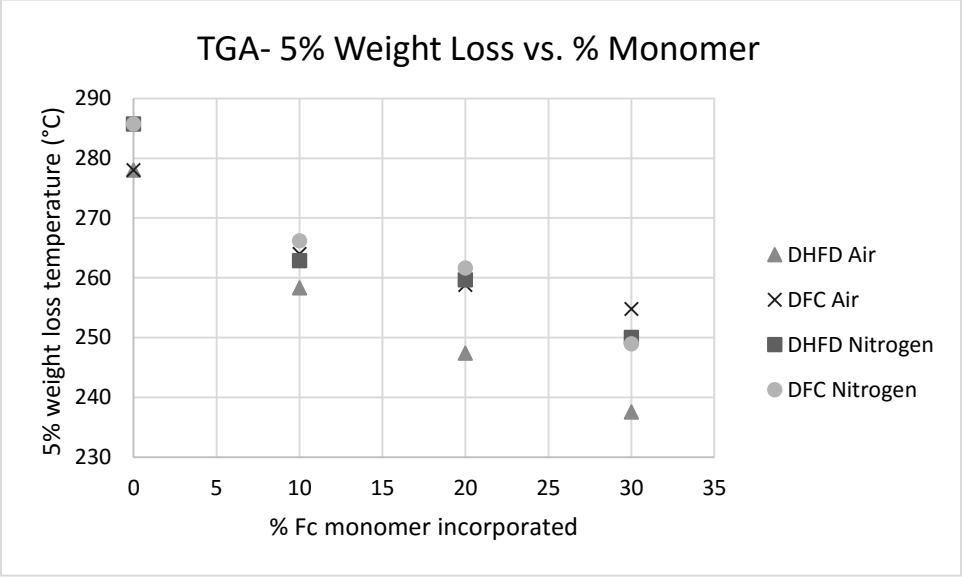

Figure 10. Plot of TGA 5% weight loss versus amount of Fc incorporation

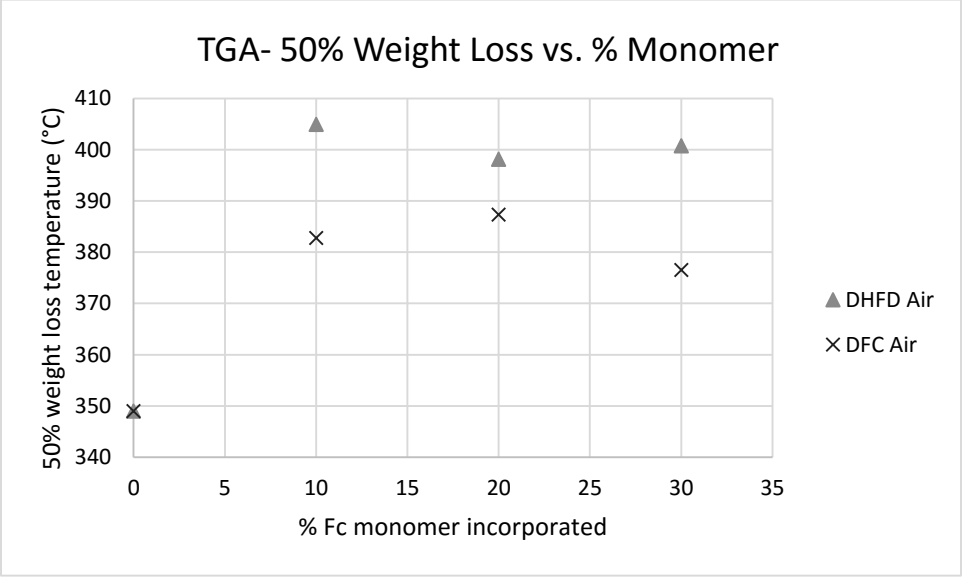

Figure 11. Plot of TGA 50% weight loss versus amount of Fc incorporation

From Figure 10 it can be seen that as ferrocene incorporation increases, the 5% degradation temperature decreases. This indicates that ferrocene is actually lowering the temperature for onset of degradation of the polymer. This may be due to the decomposition of some of the bonds holding the ferrocene into the polymer, followed by sublimation of the ferrocene. Figure 11 shows that the ferrocene incorporation significantly increases the 50% degradation temperature, although not in a linear fashion. This is notable because with any loading of ferrocene into the film the 50% degradation temperature is significantly higher than that of that of the control in the absence of Fc.

TPO was incorporated into polyurethane films at 5%, 10%, and 15% in conjunction with ferrocene monomers at 10%, 15%, and 20% to give a range of combinations. These thin films were tested using TGA in nitrogen and air, but as air is the medium in which flame retardants are needed it was the main focus. Figure 12 below and Figure 13 on the following page show contour plots for the results of the char yield in air of DFC and DHFD respectively; these were made using Minitab™ software.

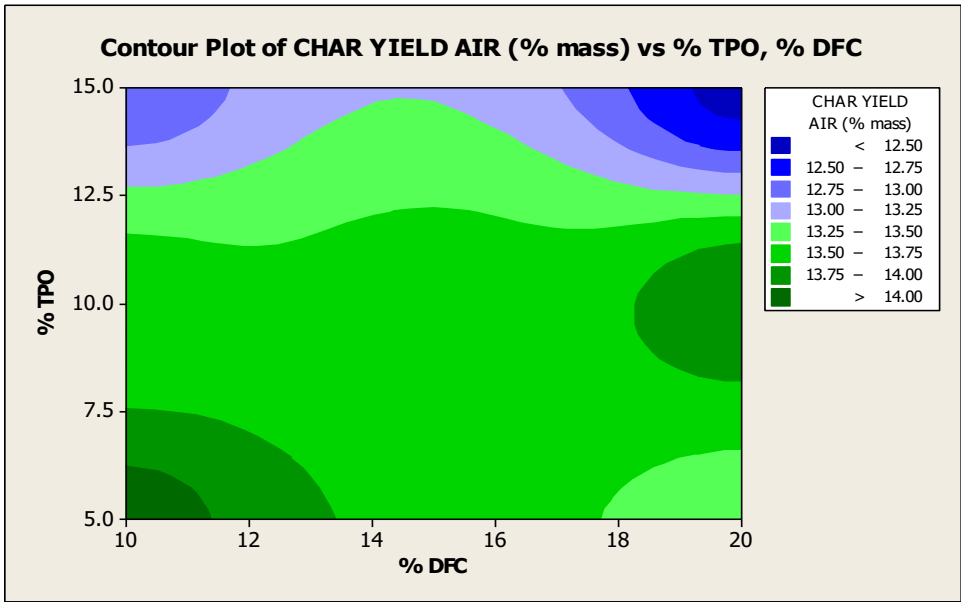

Figure 12. Contour plot of char yield in air vs % TPO and % DFC

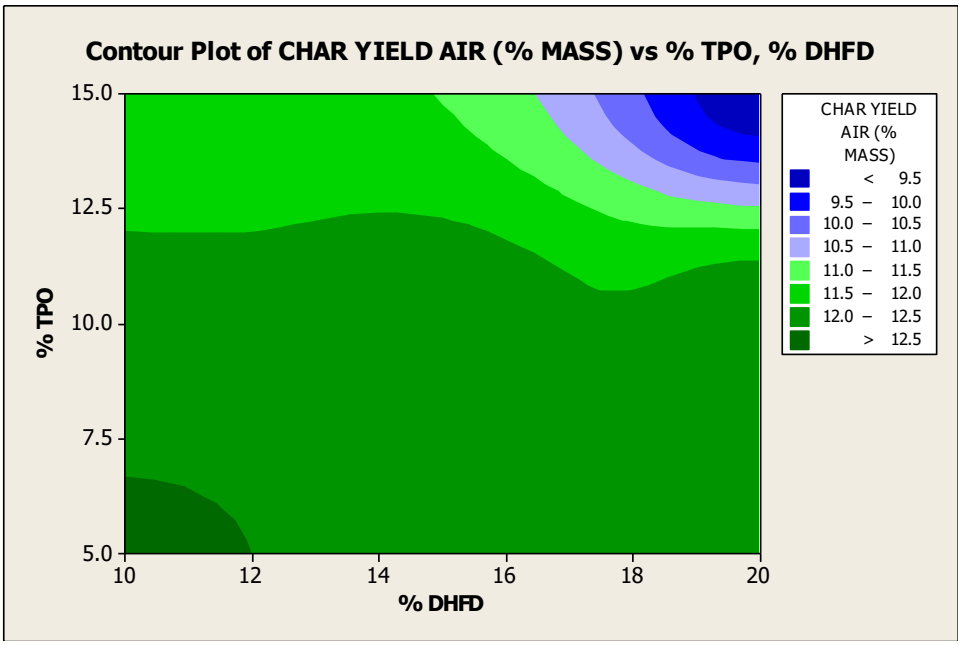

Figure 13. Contour plot of char yield in air vs % TPO and % DHFD

These contours showed similar trends as films containing Fc monomers but no TPO. As the amount of Fc or TPO increased, char yield decreased. For TPO this was expected since it was not bonded into the polymer matrix. However, the lower char yield for the polymers containing Fc monomers may suggest that the monomers have a lower thermo-oxidative stability resulting in earlier degradation and subsequent sublimation of the ferrocene at elevated temperatures.

The 5% and 50% degradation temperatures of the TGA were recorded, but the 5% showed similar effects as the Fc-only films, and decreased in temperature with an increase in TPO or Fc, likely due to early degradation of the bonds in the Fc monomers, followed by sublimation of the ferrocene. Figures 14 and 15 on the following page show contour plots for the results of 50% degradation temperature for DFC and DHFD respectively.

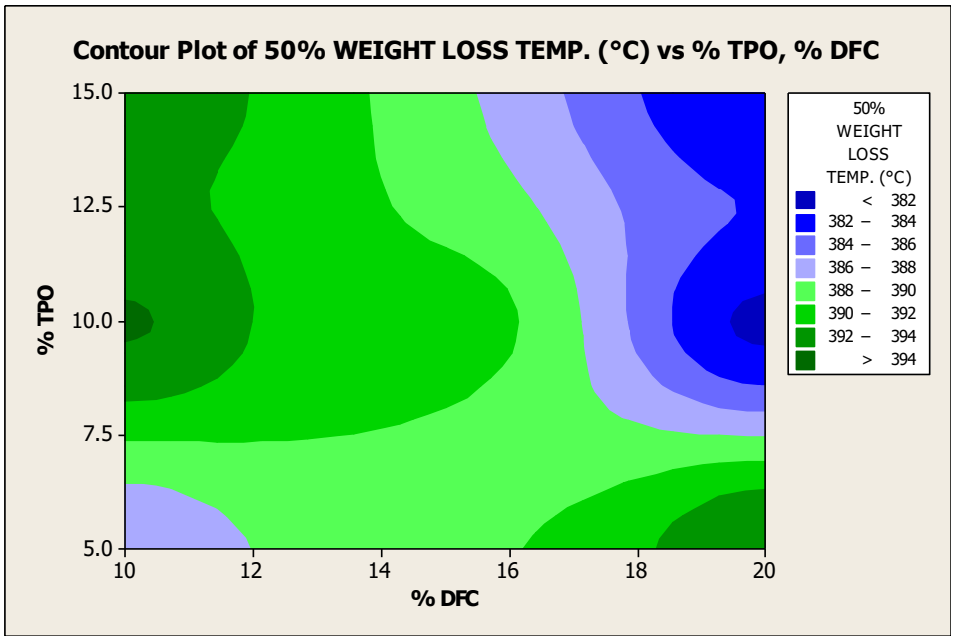

Figure 14. Contour plot of 50% degradation in air vs % TPO and % DFC

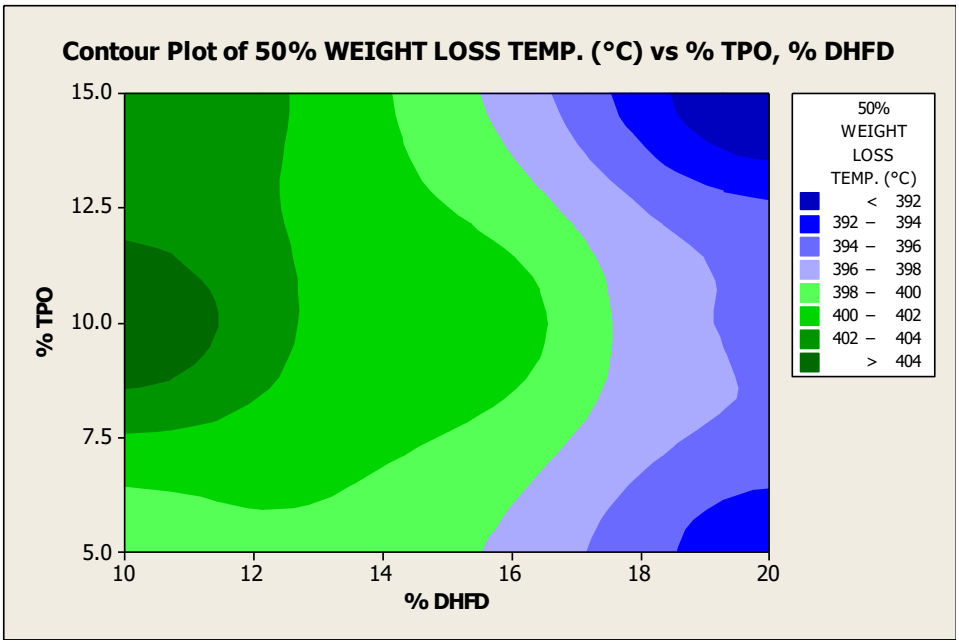

Figure 15. Contour plot of 50% degradation in air vs % TPO and % DHFD

It is noteworthy that the control sample 50% weight loss was found to be 349.0°C, significantly lower than all of the data for either DFC or DHFD. In both monomers the best location for thermal stability at 50% appears to be with 10% of each

additive, with additional additives lowering it. DFC has a lower range of 50% degradation temperature than DHFD, which could be due to the fact that there are fewer bonds holding the Fc compound into the polymer on the DFC.

3.5 Burn Test

Burn tests were conducted on thin films 5 inches long with previously mentioned quantities of ferrocene monomers incorporated into them. These tests consisted of igniting one end of the film with a Bunsen burner and holding the ignition for 10 seconds, letting the film burn to completion, and recording the burn time as well as burn distance.

The burn rate and burn distance was determined for two to four samples of each material and then averaged. Figure 16 below and Figure 17 on the following page show the burn rate and burn distance for materials containing DFC and DHFD, respectively. The control film is indicated at the 0% Fc monomer incorporation

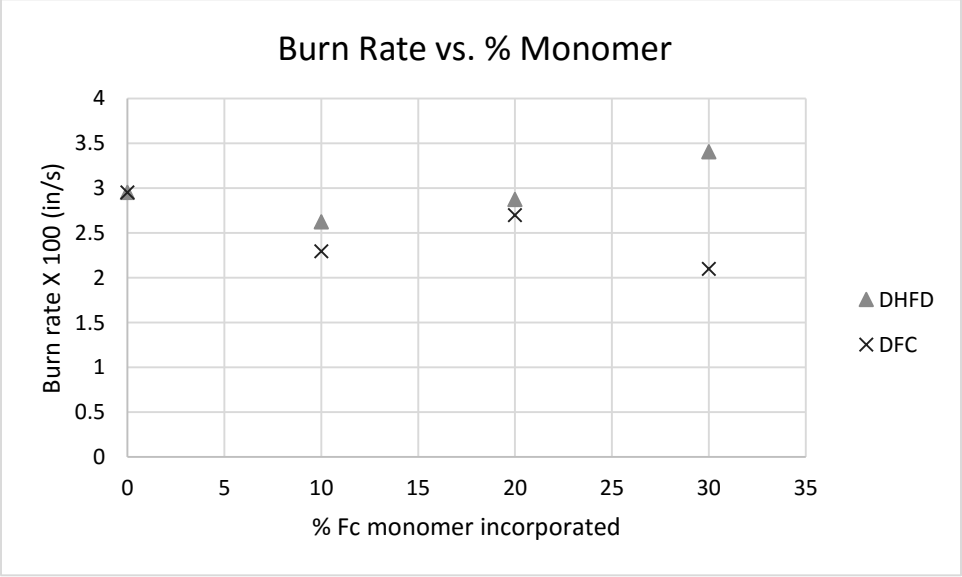

Figure 16. Plot of burn rate versus amount of Fc incorporation

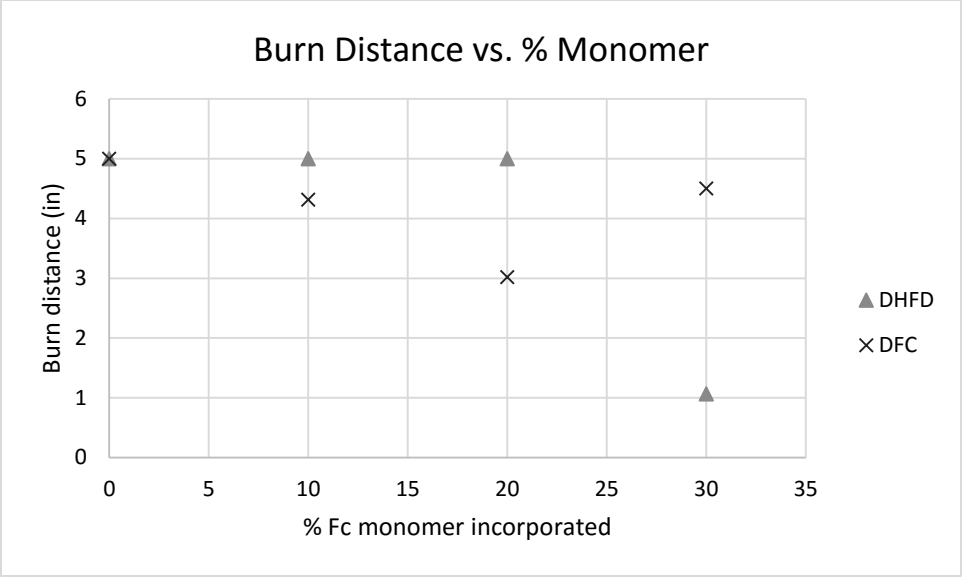

Figure 17. Plot of burn distance versus amount of Fc incorporation

Burn rate of the DFC-incorporated films consistently stayed lower than the control, although in a similar fashion to the TGA, there was a deviation from the expected trend of slowing down with more DFC at 20%. This deviation may have been due to an improper technique in a limited number of trials, however the deviation from linearity is minimal, and the overall result is still slower than that of the control film. The average burn distance for DFC also was always less than the control film, containing only the standard polyol and isocyanate components. Some of the films containing DFC burned the complete 5 inches, however at least one of each Fc loading quantity resulted in a self-extinguishing burn test. This is indicative of FR properties being added to the film by the incorporation of the DFC monomer, even at relatively low concentrations.

Burn rate of the DHFD incorporated films was lower than the control on all but the 30% loading. Although this would seem counterintuitive, the 30% samples only burned for an average of 1.1 inches before self-extinguishing. This limited result is

skewed as approximately one-third of the burn time was subject to the Bunsen burner flame. The average burn rate of a control film 1.1 inches in length was found to be 0.045in/s, which is significantly faster than the average value for the 30% loading of 0.034in/s. Burn length of the DHFD films resulted in less distinct results, as only one of the 3 films, the 30%, self-extinguished. The other two burned the full length but at a slightly slower rate.

The TPO and ferrocene incorporated films were also subjected to burn testing under the same methods. All of the films tested had at least one film self-extinguish prior to complete combustion. Burn distance was determined to be the best to use for comparison of the differing weight percentages as burn rate varies significantly in the shorter burning films. Contour plots of the burn distance as a function of TPO and ferrocene are shown below for DFC in Figure 18 and on the following page for DHFD in Figures 19.

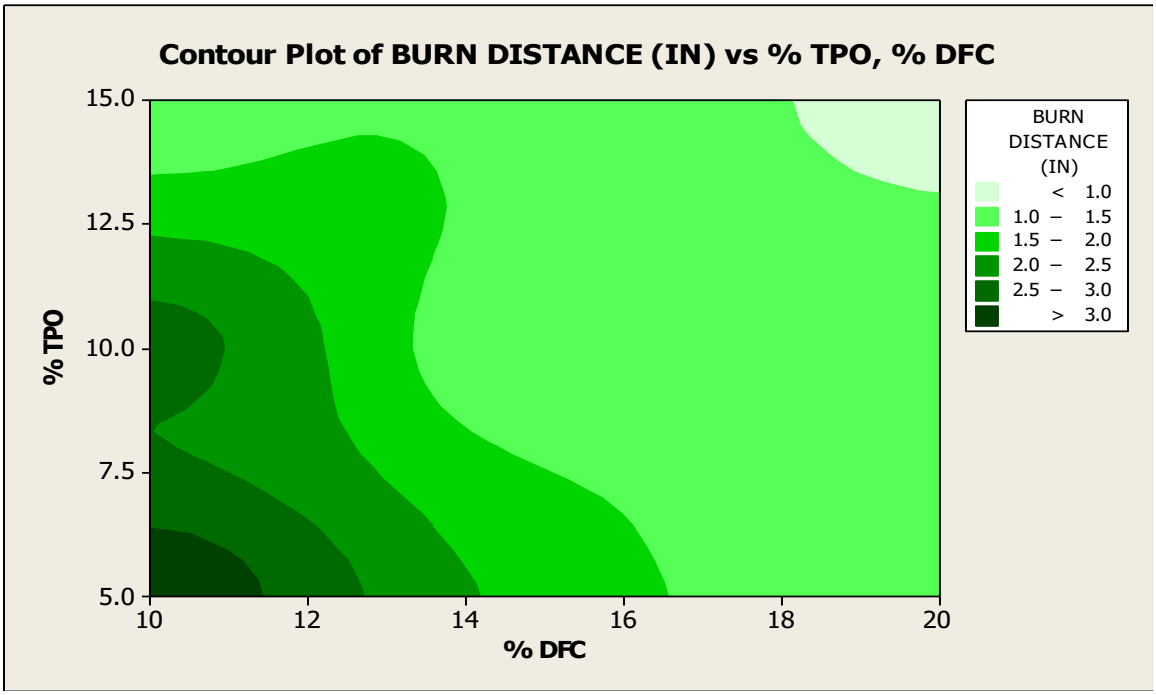

Figure 18. Contour plot of burn distance vs % TPO and % DFC

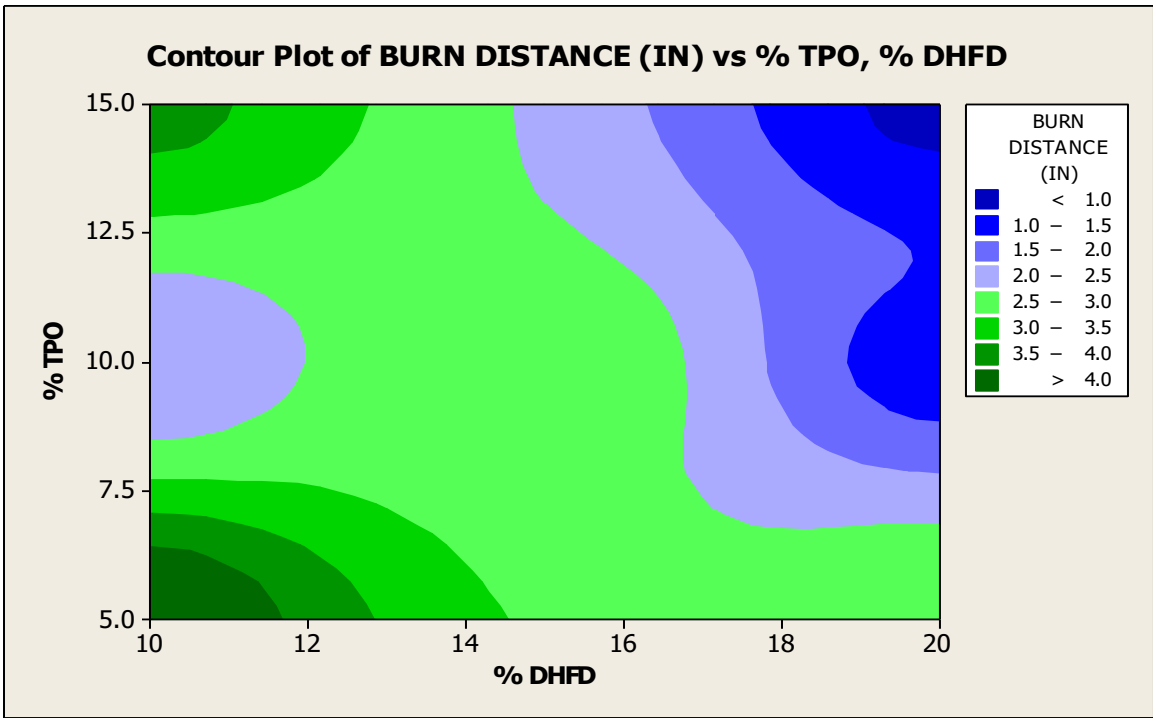

Figure 19. Contour plot of burn distance vs % TPO and % DHFD

Both monomers resulted in burn lengths that decreased as quantity of Fc or TPO increased. These results show that although there may not be synergistic effects between TPO and Fc, they both increase the flame retardant capacity of the polyurethane films. This result is consistent with TGA char yield data in that Fc is showing vapor phase flame retardant properties far more than the char method. Because both TPO and Fc are working in the vapor phase, the effects of these two different compounds eliciting the same response would not normally be expected to be synergistic, but additive at best, as was observed from the results seen in both Figures 18 and 19.

DFC/TPO films with loadings (w/w) greater than 10% TPO and 15% DFC were tacky, suggesting improper curing. This likely resulted from a slower polymerization due to a dilution effect by the TPO. When burn testing was attempted on some of these thin

films, they frequently did not ignite well. This resulted in a lower number of conclusive burn tests being averaged and a less certain result.

In addition, DHFD/TPO combinations at 20% loading of DHFD with 10% and 15% loading of TPO showed promising results for future research as thermal barrier coatings. These films held the flame to the underside of the film for a few seconds and primarily burned only along the bottom and edges of the film prior to rapid self-extinguishing.

3.6 VOC Testing

Testing for volatile organic compounds (VOCs) was performed using a gas chromatography-mass spectrometer (GC-MS). Selected samples, shown in Table 1 below, were placed in glass tubes that would only allow vapors into the column upon heating. These samples were programed to be heated to 100°C, 200°C, and 300°C, while being held at constant temperature briefly at each point. This test allows anything volatile to be removed from the sample, released into the column, and detected by the mass spectrometer.

Type	Notation
Control	mg-90-Q
Control, 15% TPO	mg-90-B
20% DFC, 15% TPO	mg-90-I
20% DHFD, 15% TPO	mg-90-P
30% DFC	mg-90-R
30% DHFD	mg-90-S

Table 1. GC-MS sample specifications

These samples were chosen in addition to the control sample as they had the largest quantities of additives. The results of the VOC testing are displayed in a GC chromatograph. There were no significant differences in any of the results, with the exception of the sample containing 30% DHFD. This tube had been recently cleaned with acetone so it had not all been evacuated properly, causing the curvature at the onset of the spectrum, as shown in Appendix B Figure S19. The large peak in the sample containing 15% TPO is believed to be contamination as this was not seen in either of the other results with TPO present; this is shown in Appendix B Figure S16. Figures 20 and 21 below show the GC chromatograph of the control as well as the 30% DFC.

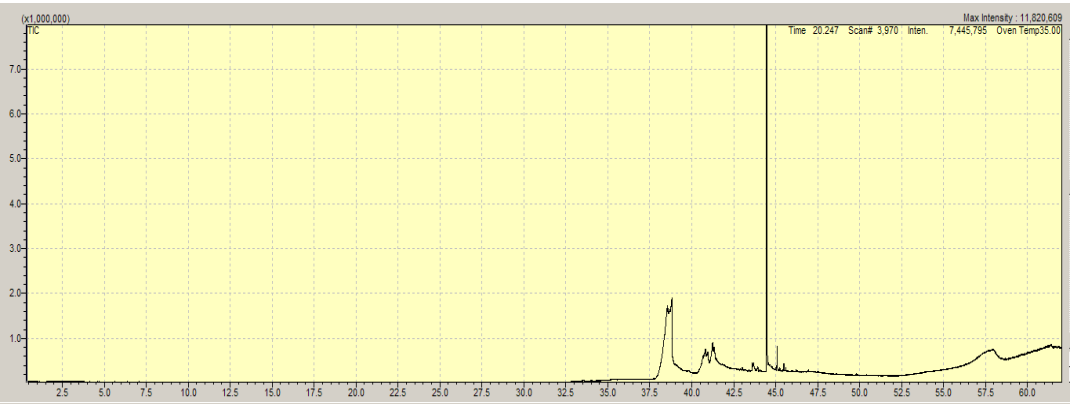

Figure 20. GC of control

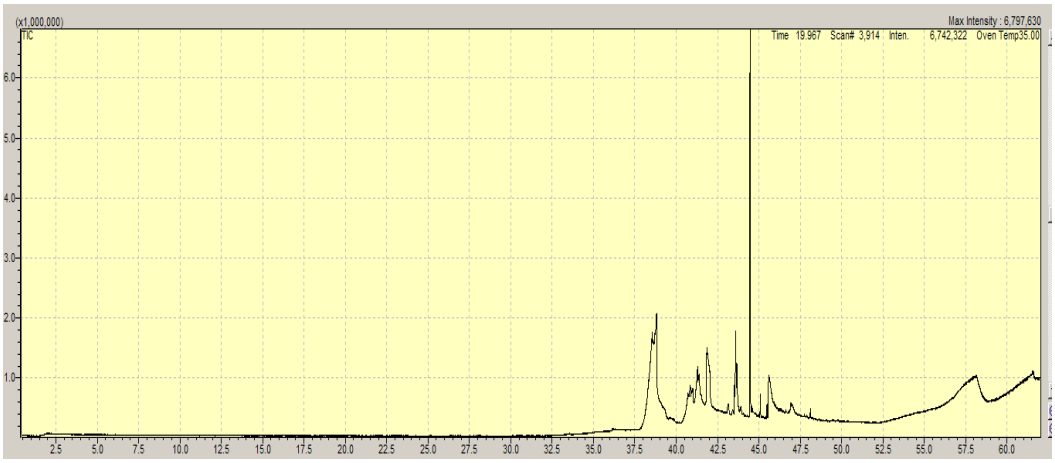

Figure 21. GC of 30% DFC

The control sample resulted in several small peaks in the 37-46 minute range, as well as one large sharp peak. In addition to this there can be seen a gradual rise in the baseline at the end of the GC near 55 minutes. This gradual rise is present both in the GC of the 30% DFC as well as the GC of the blank tube in Appendix B Figure S20, showing that it was likely not from the sample. The peaks in Figure 19 correlate closely to the peaks in the control, being in the same range. There are some small additional peaks that appear in the same time frame, 37-46 minutes, however by comparison to the overall intensity of the peaks that are in both chromatographs the significance is minimal.

Although compounds are clearly released during the heating process the crucial part of this test is that they remain constant in comparison to the neat film so that it can confidently be stated that the Fc additive, as well as the TPO in combination with Fc, does not significantly contribute to VOCs. The remainder of the chromatographs are in Appendix B, Figures S16-S20.

Chapter IV

4. Conclusion

Synthesis of the DFC and DHFD monomers was achieved by addition of glycidol to ferrocene carboxylic acid and ferrocene dicarboxylic acid respectively using TBAC as a catalyst in IPA. These reaction vessels were then heated to reflux for 16.5 and 23.5 hours, followed by addition of activated charcoal, vacuum filtration through Celite® and drying over magnesium sulfate to yield a combination of multiple isomers. The major challenge to purification and characterization was the presence of regioisomers in the DFC, and regioisomers as well as diastereomers in the DHFD. This caused ^{1}H-NMR spectroscopy to give unclear results for peak assignment, however broad integration yielded expected results for the compounds. ^{1}H-NMR, ^{13}C-NMR and FT-IR spectra were consistent with an isomer mixture of the anticipated products.

DFC and DHFD incorporated into polyurethane films in the absence of TPO resulted in some self-extinguishing samples as well as several that burned to completion, while all films containing any quantity of both TPO and Fc self-extinguished in a statistically relevant number of trials. When TGA data is considered in conjunction with the burn data, Fc monomers appear to be useful for flame retardant effects in the vapor phase primarily, due to the reduction in char as Fc is increased. These properties are not inherently synergistic with TPO, but both compounds appear to increase the FR

properties of the films that were cast. This leads to the conclusion that they are both acting in the vapor phase, which would tend towards less synergistic and more additive effects on the FR properties. These Fc/TPO films clearly show trends indicating potential usefulness for FR, however more conclusive research will be needed to determine the best potential use.

DSC results, which are shown in Appendix B, gave no significant difference in appearance from films without Fc additives incorporated, so it can be concluded that Fc additives in polyurethane films had little to no effect on the glass transition temperatures or the energy associated with that transition.

VOC results also showed minimal differences in the chromatographs of films with additives by comparison to the control, with the exception of those previously mentioned and explained in section 3.6. Fc and TPO added little to no additional volatile compounds to the films. This is ideal as sublimation of the FR compounds from the film below a reasonable temperature would result in ineffective FR after removal of those compounds.

4.1 Future Research

Although much data was gathered in this study, there remain many tests and optimizations that should be accomplished to better understand these modified polyurethanes. Cone calorimetry is a common instrumental technique for FR testing, but one was not accessible at the time of this study. Polyurethane foams one of the major products of polyurethane industry and they should be explored with here described Fc components to see if they show promise outside of thin film application. These monomers also have the potential to be incorporated into any other polymer resin that

uses alcohols as one of the functional groups needed, such as polyesters, or the alcohol functionalities could be modified for application in other resins.

The synthesis of monomers could also be explored more in an attempt to optimize one regioisomer or the other. This optimization could result in an increased reactivity of the alcohols should it be possible to shift the reaction towards the synthesis of the regioisomers containing only primary alcohols, DFC-B and DHFD-C. This could allow for better crosslinking into the polyurethane structure allowing the addition of more FC to the films without compromising structural properties.

REFERENCES

1. Lu, S.-Y.; Hamerton, I. Recent Developments in the Chemistry of Halogen-Free Flame Retardant Polymers. *Progress in Polymer Science*. **2002**, *27*, 1661–1712.
2. Troitzsch, J. H. Overview of Flame Retardants. *Chemistry Today*. **1998**, *16*.
3. Najafi-Mohajeri, N.; Nelson, G. L.; Benrashid, R. Synthesis and Properties of New Ferrocene-Modified Urethane Block Copolymers. *Journal of Applied Polymer Science.* **2000**, *76*, 1847–1856.
4. Weil, E. D.; Levchik, S. V. Commercial Flame Retardancy of Polyurethanes. *Journal of Fire Sciences*. **2004**, *22*, 183–210.
5. Morgan, A. B.; Wilkie, C. A. *Non-Halogenated Flame Retardant Handbook*; Scrivener Publishing: Beverly, MA, 2014.
6. Mehdipour-Ataei, S.; Babanzadeh, S. New Types of Heat-Resistant, Flame-Retardant Ferrocene-Based Polyamides with Improved Solubility. *Reactive and Functional Polymers*. **2007**, *67*, 883–892.
7. Zhou, K.; Zhang, Q.; Liu, J.; Wang, B.; Jiang, S.; Shi, Y.; Hu, Y.; Gui, Z. Synergetic Effect of Ferrocene and MoS2 in Polystyrene Composites with Enhanced Thermal Stability, Flame Retardant and Smoke Suppression Properties. *RSC Adv.* **2014**, *4*, 13205–13214.
8. Verreault, J.; Gabrielsen, G. W.; Chu, S.; Muir, D. C. G.; Andersen, M.; Hamaed, A.; Letcher, R. J. Flame Retardants And Methoxylated and Hydroxylated Polybrominated Diphenyl Ethers in Two Norwegian Arctic Top Predators: Glaucous Gulls and Polar Bears. *Environmental Science & Technology*. **2005**, *39*, 6021–6028.

9. Eskenazi, B.; Chevrier, J.; Rauch, S.; Kogut, K.; Harley, K.; Johnson, C.; Trujillo, C.; Sjödin, A.; Bradman, A. In Utero and Childhood Polybrominated Diphenyl Ether (Pbde) Exposures and Neurodevelopment In The Chamacos Study. *Environmental Health Perspectives*. **2013**, *121*, 285–304.
10. Linteris, G. T.; Rumminger, M. D.; Babushok, V. Flame Inhibition by Ferrocene, Alone and with CO2 and CF3H. In *Halon Options Technical Working Conference*; HOTWC Publications: Albuquerque, NM, 2000.
11. Reeves, P. C. Carboxylation Of Aromatic Compounds: Ferrocenecarboxylic Acid. *Org. Synth.* **1977**, *56*, 28–31.
12. Vogel, M., Rausch, M., Rosenberg, H.; *Journal of Organic Chemistry*. **1957**, 22, 1016.
13. Knobloch, F. W.; Rauscher, W. H. Condensation Polymers of Ferrocene Derivatives. *Journal of Polymer Science.* **1961**, *54*, 651–656.
14. Gong, C.; Fréchet, J. M. J. Proton Transfer Polymerization in the Preparation of Hyperbranched Polyesters with Epoxide Chain-Ends and Internal Hydroxyl Functionalities. *Macromolecules*. **2000**, *33*, 4997–4999.
15. Silverstein, R. M.; Webster, F. X.; Kiemle, D. J. *Spectrometric Identification of Organic Compounds*; 8th ed.; Wiley: New Delhi, 2015.

APPENDIX

APPENDIX A

^{1}H-NMR, ^{13}C-NMR, FT-IR SPECTRA, and DSC

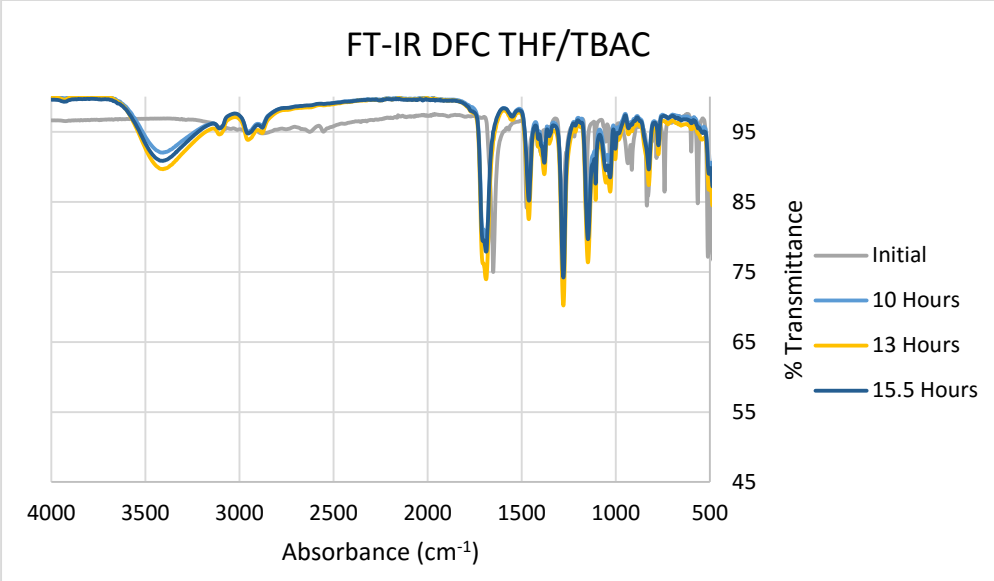

Figure S1. FT-IR spectrum of DFC at varying reaction times in THF/TBAC

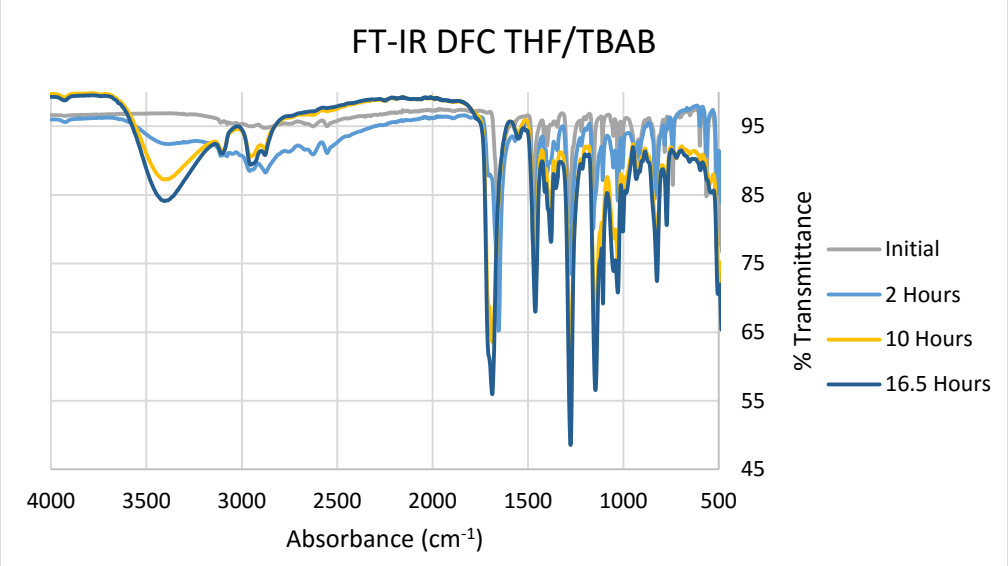

Figure S2. FT-IR spectrum of DFC at varying reaction times in THF/TBAB

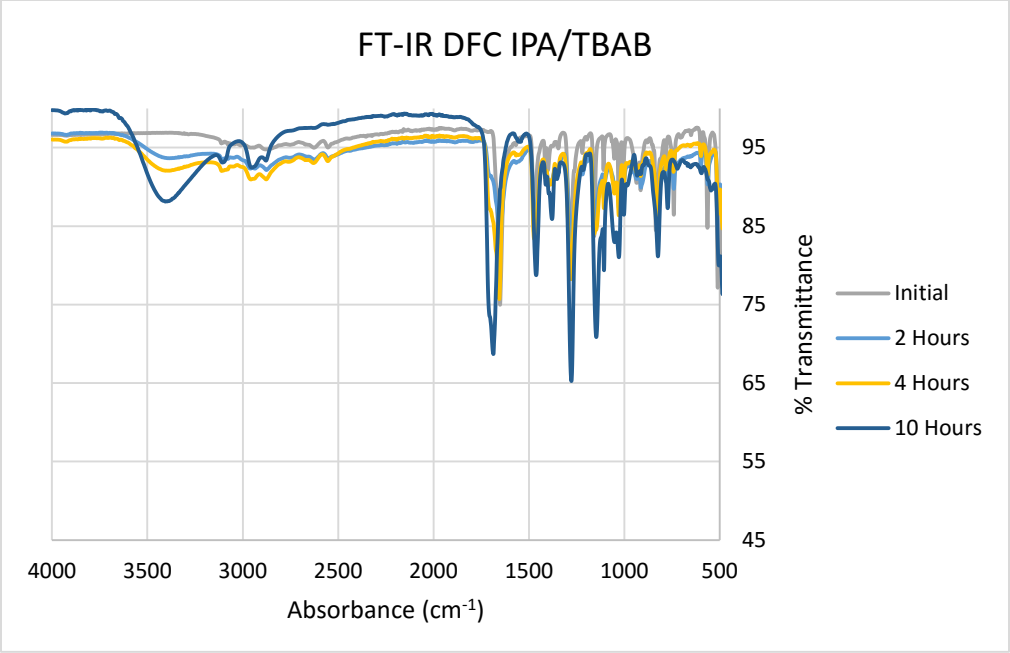

Figure S3. FT-IR spectrum of DFC at varying reaction times in IPA/TBAB

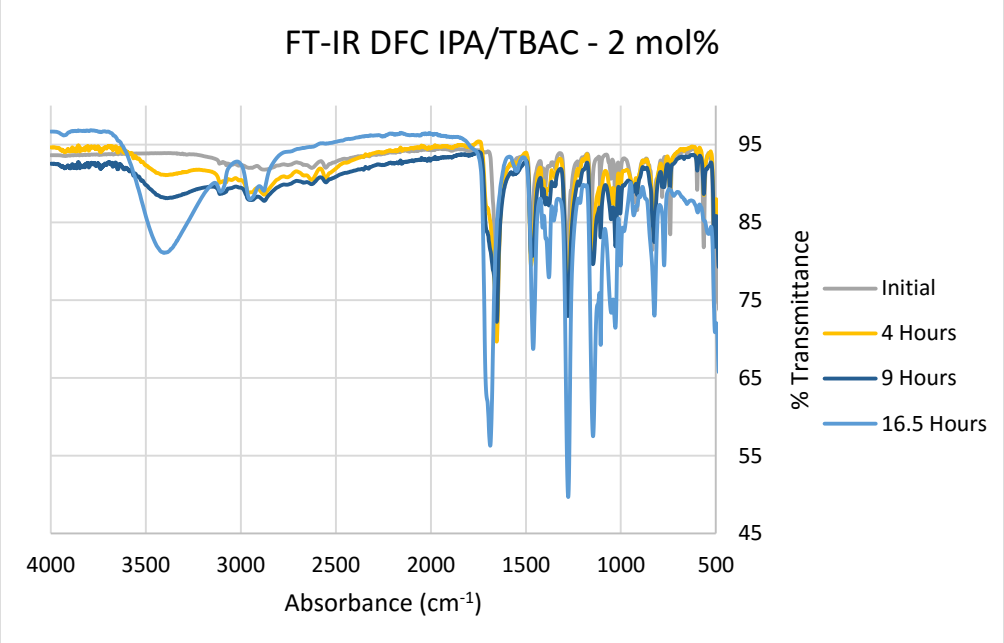

Figure S4. FT-IR spectrum of DFC at varying reaction times in IPA with 2 mol% TBAC

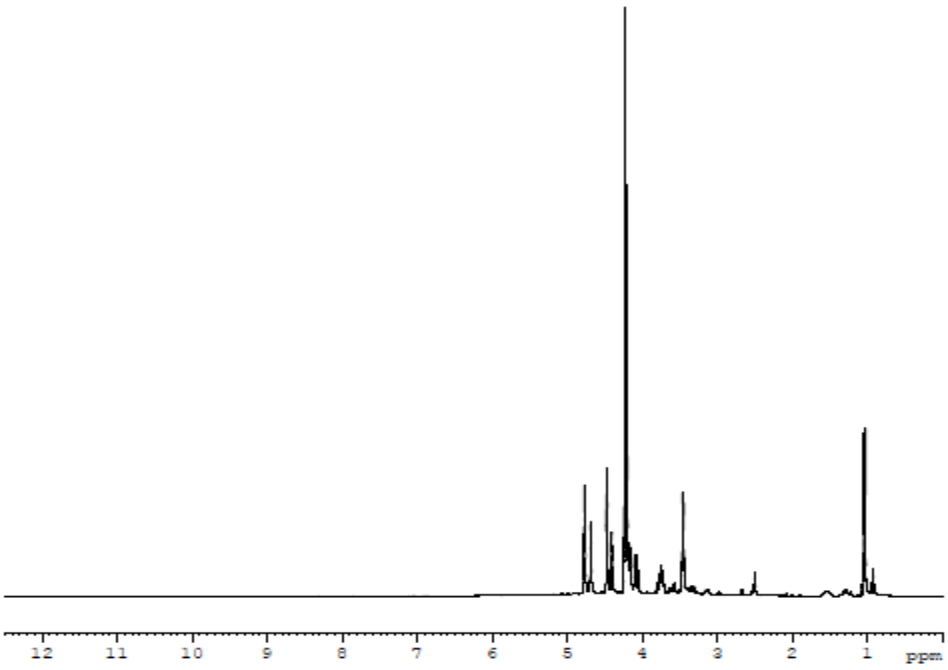

Figure S5. Full ^{1}H NMR spectrum of DFC

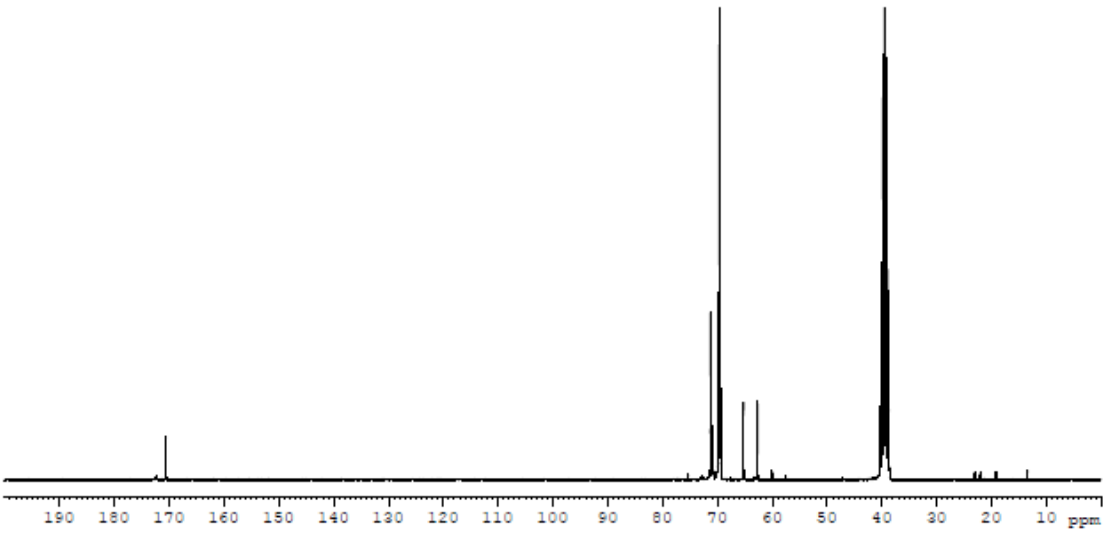

Figure S6. Full ^{13}C NMR spectrum of DFC

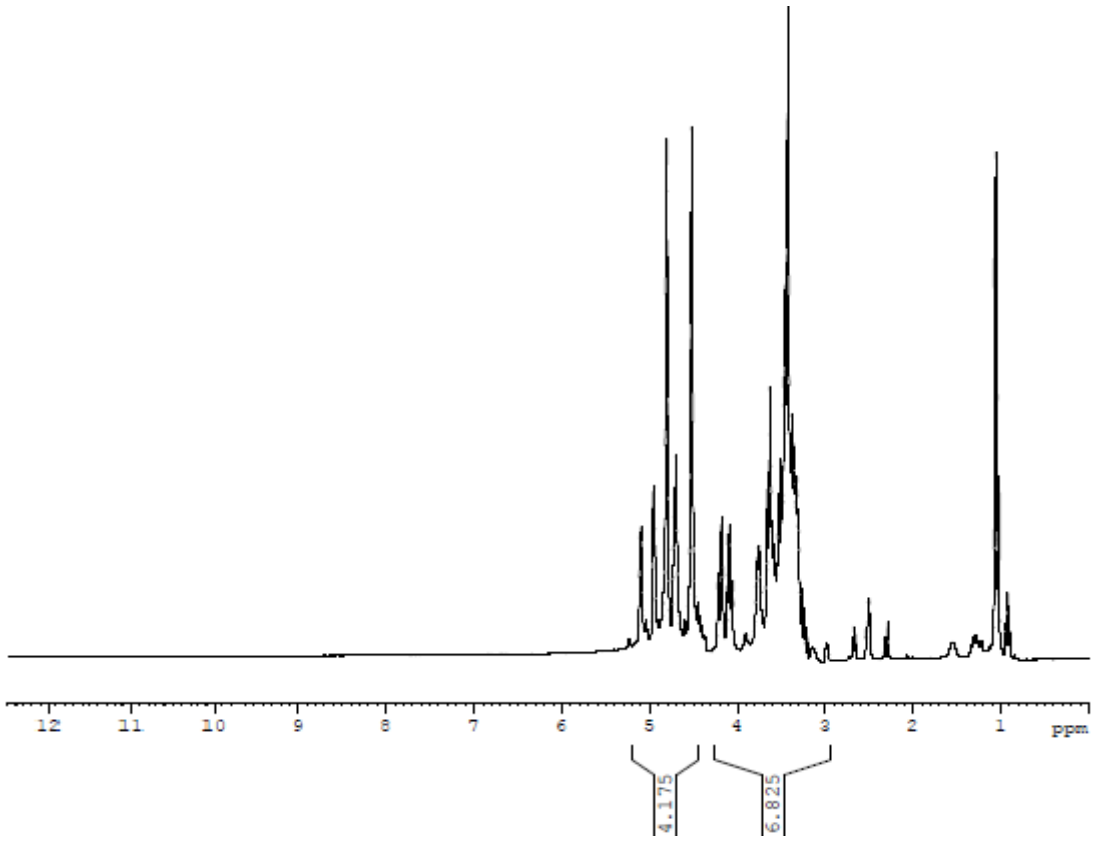

Figure S7. Full ^{1}H NMR spectrum of DHFD

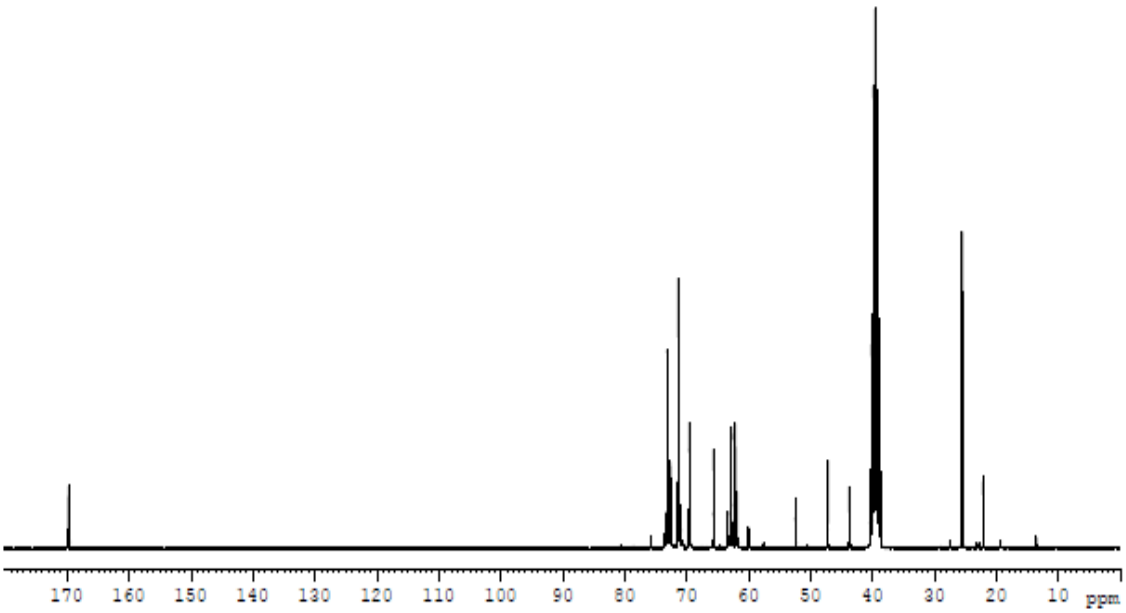

Figure S8. Full ^{13}C NMR spectrum of DHFD

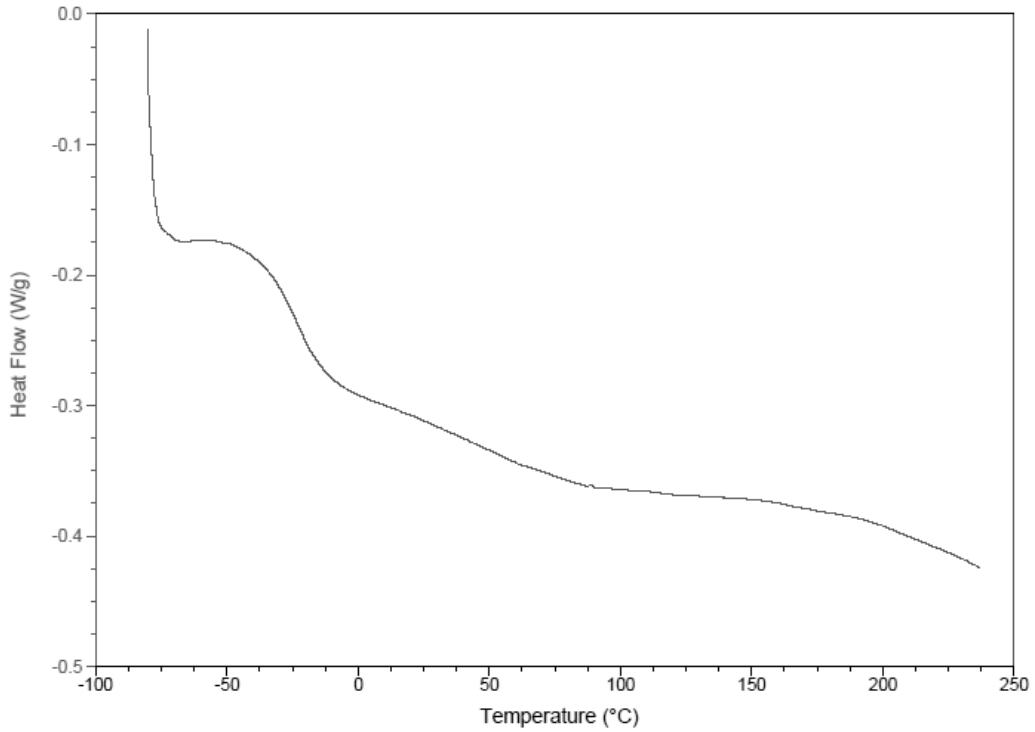

Figure S9. DSC of control film

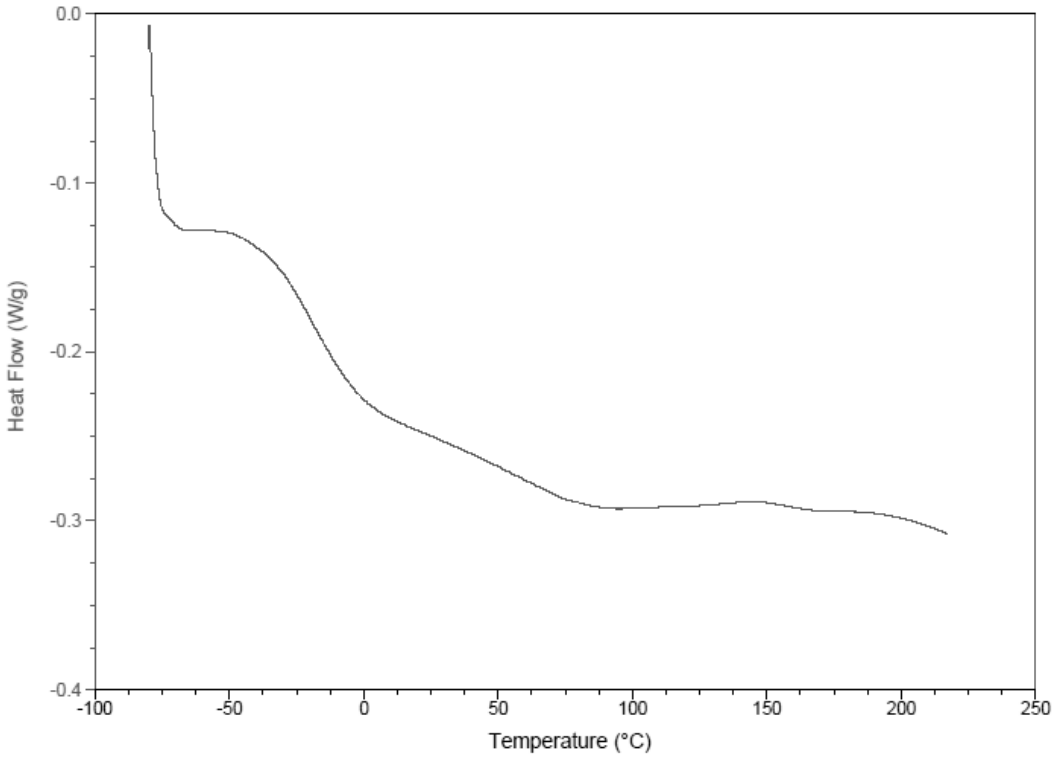

Figure S10. DSC of film with 10% DFC

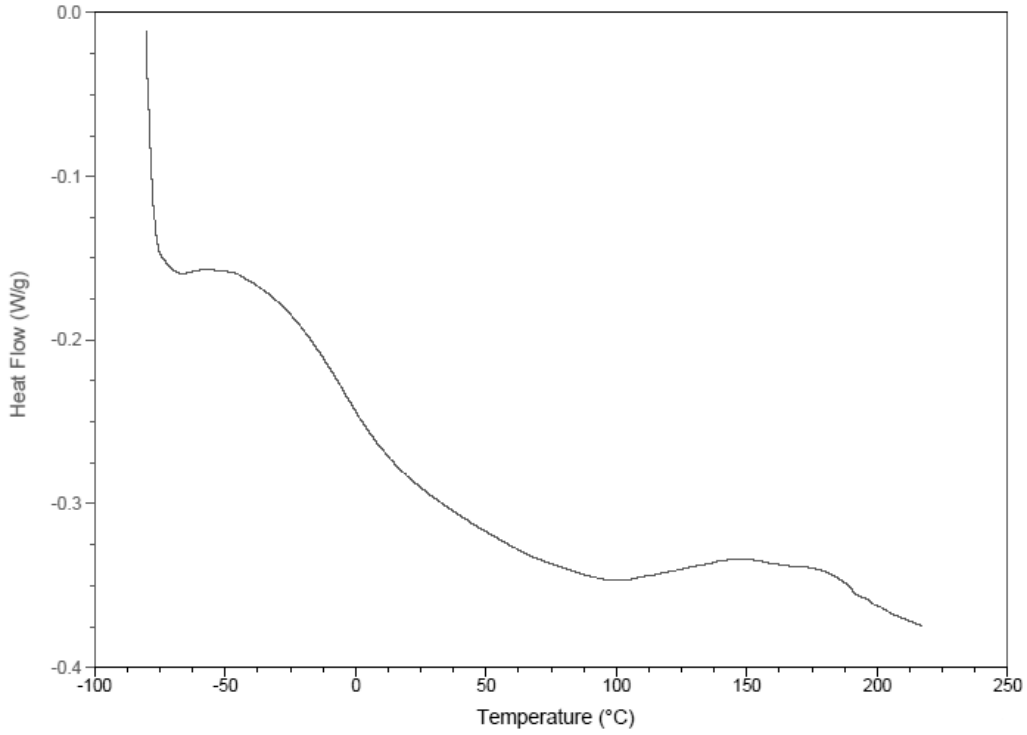

Figure S11. DSC of film with 20% DFC

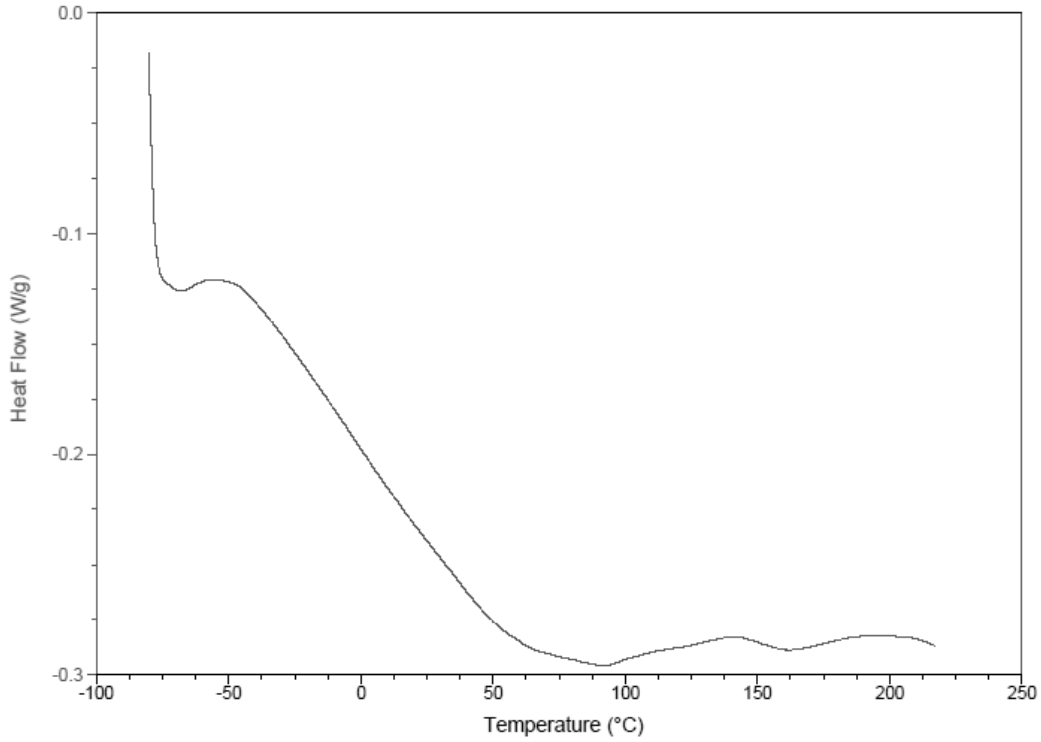

Figure S12. DSC of film with 30% DFC

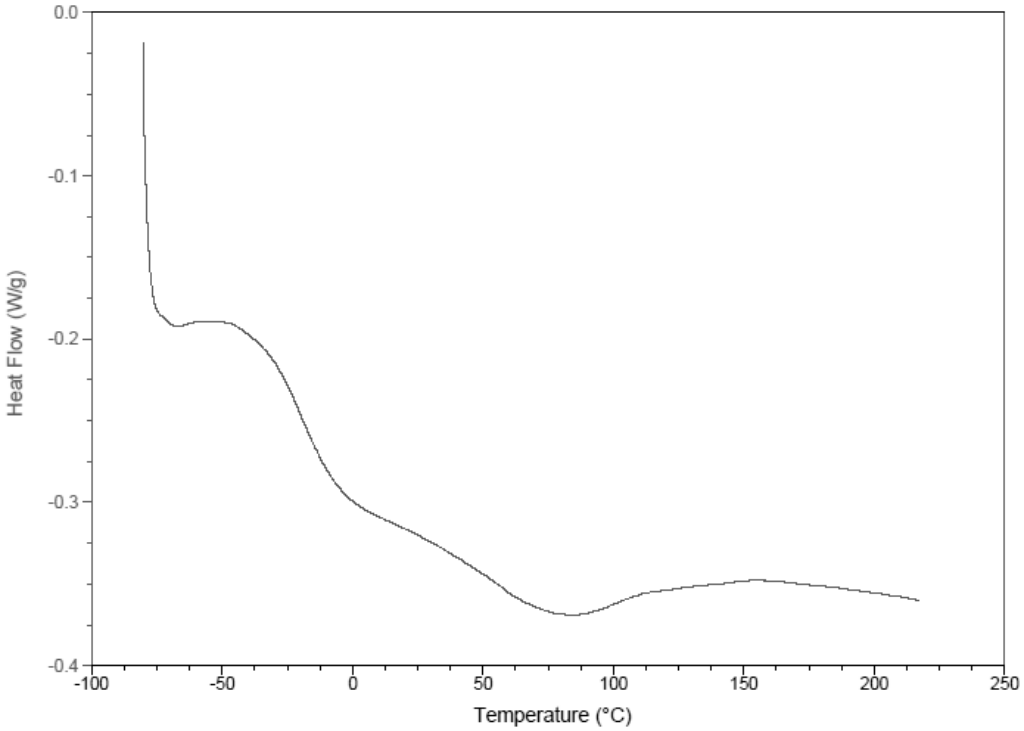

Figure S13. DSC of film with 10% DHFD

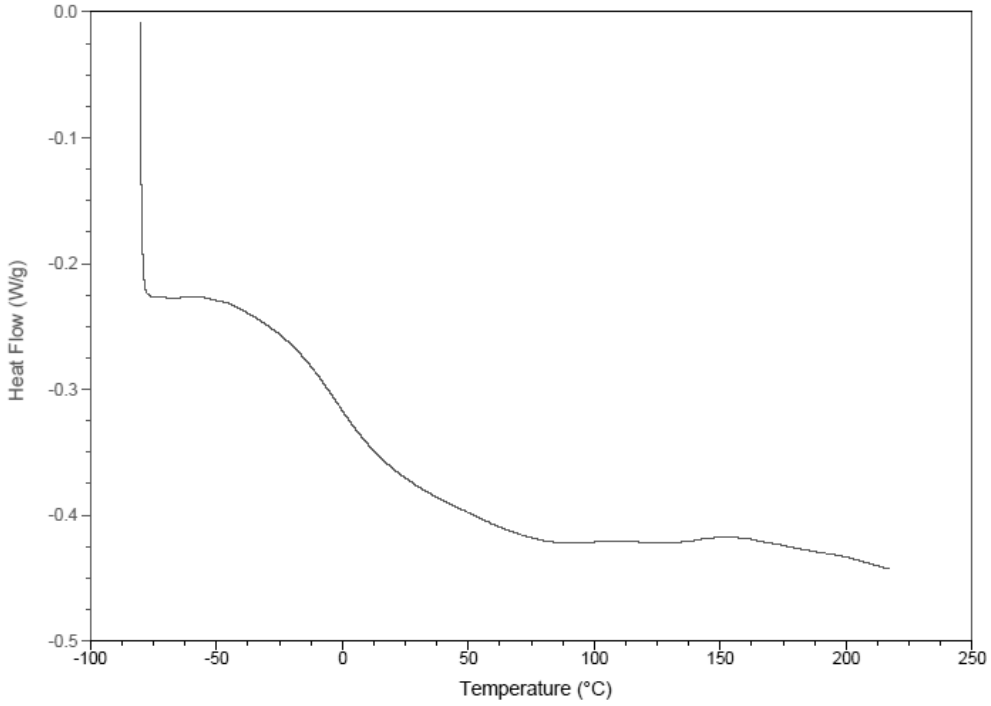

Figure S14. DSC of film with 20% DHFD

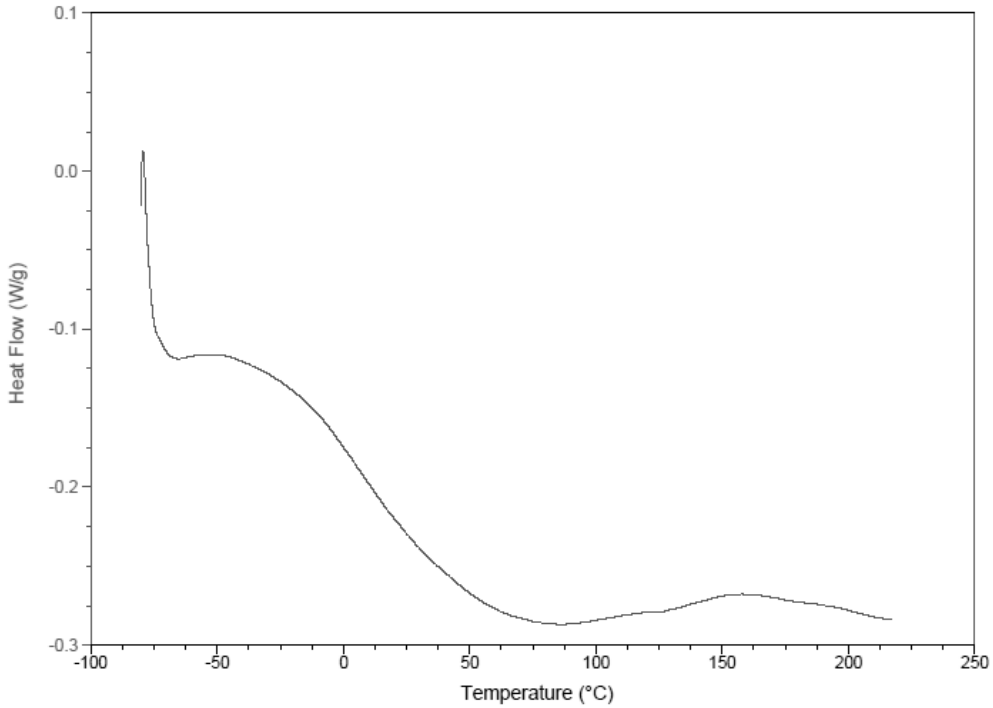

Figure S15. DSC of film with 30% DHFD

APPENDIX B

VOC RESULTS

S16. GC of 15% TPO

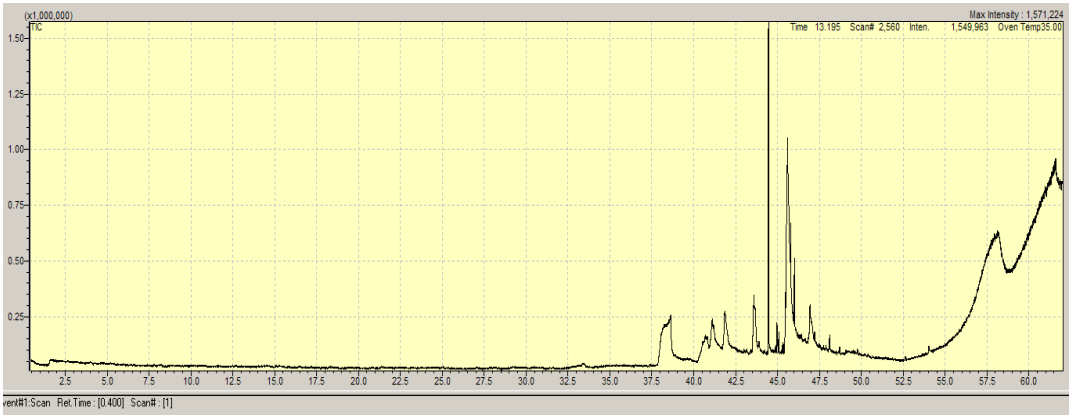

S17. GC of 15% TPO and 20% DFC

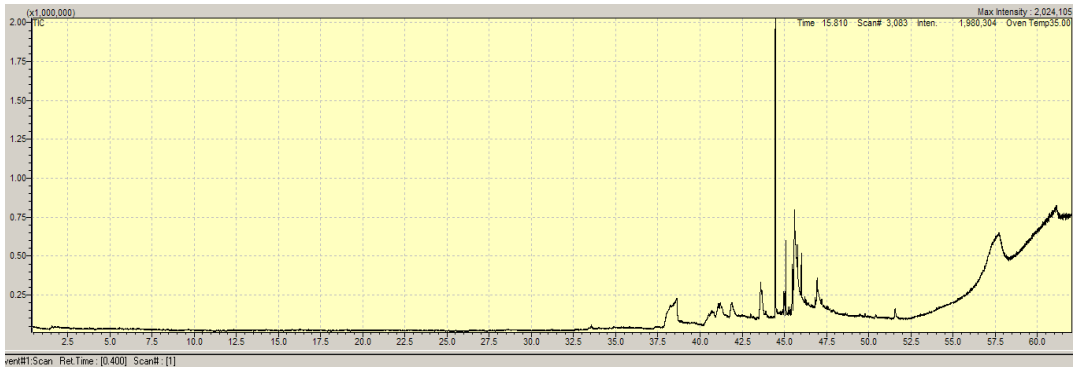

S18. GC of 15% TPO and 20% DHFD

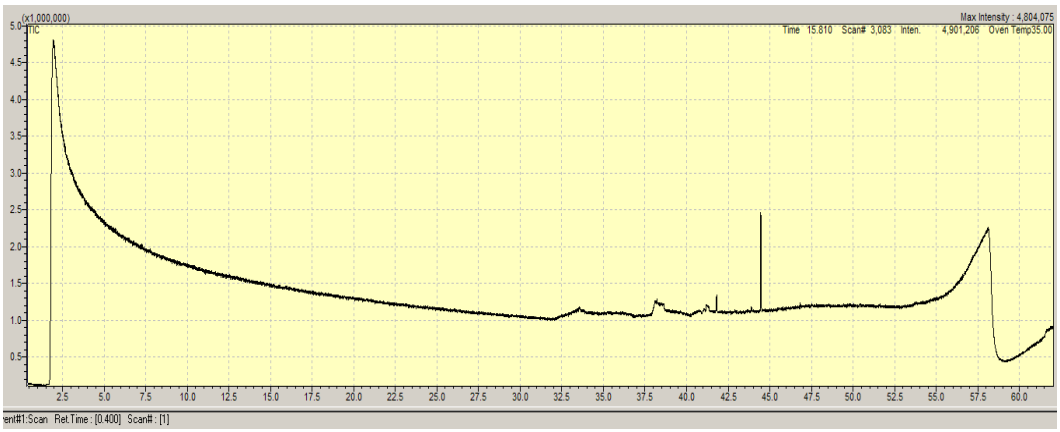

S19. GC of 30% DHFD

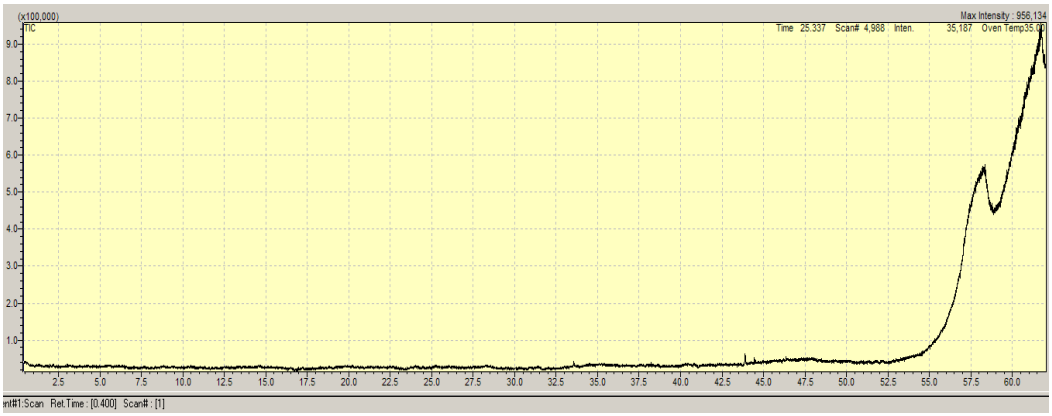

S20. GC of empty tube